

This is a repository copy of *Superoxide is promoted by sucrose and affects amplitude of circadian rhythms in the evening*.

White Rose Research Online URL for this paper:

<https://eprints.whiterose.ac.uk/171935/>

Version: Accepted Version

---

**Article:**

Roman-Fernandez, Angela, Li, Xiang, Deng, Dongjing et al. (4 more authors) (2021) Superoxide is promoted by sucrose and affects amplitude of circadian rhythms in the evening. Proceedings of the National Academy of Sciences of the United States of America. e2020646118. ISSN 1091-6490

<https://doi.org/10.1073/pnas.2020646118>

---

**Reuse**

Items deposited in White Rose Research Online are protected by copyright, with all rights reserved unless indicated otherwise. They may be downloaded and/or printed for private study, or other acts as permitted by national copyright laws. The publisher or other rights holders may allow further reproduction and re-use of the full text version. This is indicated by the licence information on the White Rose Research Online record for the item.

**Takedown**

If you consider content in White Rose Research Online to be in breach of UK law, please notify us by emailing [eprints@whiterose.ac.uk](mailto:eprints@whiterose.ac.uk) including the URL of the record and the reason for the withdrawal request.

1

2 **Main Manuscript for**

3 Superoxide is promoted by sucrose and affects amplitude of circadian  
4 rhythms in the evening

5 Ángela Román<sup>a,b,1,2</sup>, Xiang Li<sup>a,1</sup>, Dongjing Deng<sup>a,1</sup>, John W. Davey<sup>b</sup>, Sally James<sup>b</sup>, Ian A.  
6 Graham<sup>b</sup>, Michael J. Haydon<sup>a,b,3</sup>

7 <sup>a</sup>School of BioSciences, The University of Melbourne, Parkville, 3010, Australia

8 <sup>b</sup>Department of Biology, University of York, Wentworth Way, YO10 5DD, United Kingdom

9 <sup>1</sup> These authors contributed equally

10 <sup>2</sup> Current address: Estación Experimental de Aula Dei – CSIC, Zaragoza, E-50059, Spain.

11 <sup>3</sup> Michael J. Haydon

12 **Email:** m.haydon@unimelb.edu.au

13 AR 0000-0003-3457-999X; XL 0000-0002-6325-6439; JWD 0000-0002-1017-9775; IAG 0000-  
14 0003-4007-1770; MJH 0000-0003-2486-9387

15 **Classification**

16 Biological Sciences; Plant Biology

17 **Keywords**

18 Circadian, superoxide, sugar, redox, ROS

19 **Author Contributions**

20 MJH conceived the study; AR, XL, DD, MJH designed experiments; AR, XL, DD, JWD, SJ, MJH  
21 performed experiments; AR, XL, DD, JWD, IAG, MJH analysed or interpreted data; MJH wrote  
22 the manuscript; all authors edited the manuscript.

23 **This PDF file includes:**

24 Main Text  
25 Figures 1 to 4

26

27

## 28 **Abstract**

29 Plants must coordinate photosynthetic metabolism with the daily environment and adapt rhythmic  
30 physiology and development to match carbon availability. Circadian clocks drive biological  
31 rhythms which adjust to environmental cues. Products of photosynthetic metabolism, including  
32 sugars and reactive oxygen species (ROS), are closely associated with the plant circadian clock  
33 and sugars have been shown to provide metabolic feedback to the circadian oscillator. Here, we  
34 report a comprehensive sugar-regulated transcriptome of Arabidopsis and identify genes  
35 associated with redox and ROS processes as a prominent feature of the transcriptional response.  
36 We show that sucrose increases levels of superoxide ( $O_2^-$ ) which is required for transcriptional  
37 and growth responses to sugar. We identify circadian rhythms of  $O_2^-$ -regulated transcripts which  
38 are phased around dusk and find that  $O_2^-$  is required for sucrose to promote expression of  
39 *TIMING OF CAB1 (TOC1)* in the evening. Our data reveal a role for  $O_2^-$  as a metabolic signal  
40 affecting transcriptional control of the circadian oscillator in Arabidopsis.

## 41 **Significance Statement**

42

43 Distinguishing the effects of light and sugars in photoautotrophic cells is challenging. The  
44 circadian system is a regulatory network that integrates light and metabolic signals and controls  
45 rhythmic physiology and growth. Our experimental approach has defined a light-independent,  
46 sugar-regulated transcriptome in Arabidopsis and revealed reactive oxygen species (ROS) as a  
47 prominent feature. ROS are by-products of photosynthetic metabolism and oscillate with circadian  
48 rhythms but have not previously been demonstrated as inputs to the plant circadian oscillator.  
49 Our data suggest a new role for superoxide as a rhythmic sugar signal which acts in the evening  
50 and affects circadian gene expression and growth.

51

52

53

## 54 **Main Text**

55

### 56 **Introduction**

57

58 Plant metabolism is inextricably linked to daily photoperiodic cycles because of the requirement of  
59 light for photosynthesis. Anticipation and adaptation to changing light availability enables plants  
60 to optimise metabolism according to their immediate environment. Plant metabolism responds to  
61 environmental cues, such as light, temperature, biotic and abiotic stress by diverse mechanisms  
62 (1).

63

64 Plant cells require signalling mechanisms to sense carbon and energy status and adjust  
65 metabolism. Snf1 RELATED KINASE 1 (SnRK1) and TARGET OF RAPAMYCIN 1 (TOR1) are  
66 counteracting signalling hubs which are activated under low and replete carbon status,  
67 respectively (2, 3). Trehalose-6-phosphate (T6P) is an essential signalling sugar which indicates  
68 carbon status and acts through SnRK1 (4, 5).

69

70 Circadian clocks are an endogenous time-keeping mechanism which regulate rhythms of  
71 physiology and metabolism and control responses to environmental signals according to the time  
72 of day (6). The core circadian oscillator in Arabidopsis is a network of transcription factors  
73 comprised of Myb-like genes *CIRCADIAN CLOCK ASSOCIATED 1 (CCA1)*, *LATE ELONGATED*  
74 *HYPOCOTYL (LHY)* and *REVIELLE (RVE)* expressed at dawn, *PSEUDO RESPONSE*  
75 *REGULATOR (PRR)* genes expressed through the day including *TIMING OF CAB 1 (TOC1)* at

76 dusk, and the Evening Complex (EC) in the night. The phase and amplitude of gene expression  
77 and protein levels are responsive to environmental cues and they, in turn, coordinate the  
78 regulation of thousands of genes.

79  
80 There is extensive transcriptional and post-transcriptional control of photosynthetic metabolism by  
81 the circadian clock and there is metabolic feedback on the circadian oscillator. Elevated SnRK1  
82 activity under carbon limitation lengthens circadian period and sucrose shortens period by T6P-  
83 SnRK1 acting on the oscillator gene *PRR7* (7–9). Period also responds to glucose by a TOR-  
84 dependent mechanism (10). In continuous dark, circadian rhythms rapidly dampen, but can be  
85 sustained by addition of sugars. This effect of sugar requires GIGANTEA (GI), a clock protein  
86 which is stabilised by sucrose in the evening (11). Sugars can also reinitiate transcriptional  
87 rhythms in dark-adapted seedlings, setting phase according to the time of sugar application (8,  
88 12), but the mechanism is unknown.

89  
90 Redox state and levels of reactive oxygen species (ROS), which are tightly linked to metabolism,  
91 are also associated with circadian rhythms in plants. There are circadian rhythms of hydrogen  
92 peroxide (H<sub>2</sub>O<sub>2</sub>) and NADP(H)<sup>+</sup> in *Arabidopsis* (13, 14). Circadian rhythms of peroxiredoxin  
93 oxidation have been detected across Kingdoms (15). These rhythms of redox state and  
94 associated ROS are generally considered as outputs of rhythmic metabolism controlled by the  
95 circadian clock (13), or even independent of the circadian oscillator (15). The defence hormone  
96 salicylic acid perturbs redox state and affects gating of immune response, dependent on the  
97 redox-sensitive transcription factor NON-EXPRESSOR OF PATHOGENESIS 1 (NPR1) (14). But  
98 there is presently no clear evidence of a role for redox signals as a mechanism of metabolic  
99 feedback to the circadian oscillator in plants.

100  
101 Distinguishing sugar and light signals can be challenging in photosynthetic cells since it is likely  
102 that sugar signalling will be activated in the light. Recent advances in our understanding of the  
103 impact of metabolic signalling to the plant circadian clock have relied on experiments in low light  
104 or darkness (7, 8, 10–12, 16). Here, we use an experimental approach based on the previous  
105 observation that sugar can activate expression of circadian clock genes in dark-adapted  
106 seedlings to define a light-independent, sugar-regulated transcriptome in *Arabidopsis* (8, 12). We  
107 compare the response of the transcriptome to sucrose in the dark and inhibition of photosynthesis  
108 in the light and identify redox and ROS processes as a prominent feature of transcriptional  
109 responses to sugars. We demonstrate that superoxide (O<sub>2</sub><sup>-</sup>) can act as a signal to alter gene  
110 expression and growth in response to sucrose. This O<sub>2</sub><sup>-</sup> signal acts to promote transcription of  
111 circadian oscillator genes in the evening. These reveal that ROS can function as metabolic  
112 signals affecting circadian rhythms in *Arabidopsis*.

113

## 114 Results

115

116 To identify transcripts that are regulated by sugars in the presence and absence of light and  
117 photosynthesis, we designed an RNA-seq experiment based on the previous observation that  
118 sugars can reinitiate transcriptional circadian rhythms in dark-adapted *Arabidopsis* seedlings (8,  
119 12). Two-week old wild-type (Col-0) seedlings were grown in the dark for 72 h to dampen  
120 circadian rhythms and establish a stabilised C starvation state. At subjective dawn, dark-adapted  
121 seedlings were transferred to media containing 10 mM mannitol (osmotic control) or sucrose and  
122 maintained in the dark or transferred to media containing 10 mM mannitol with or without 3-(3,4-  
123 dichlorophenyl)-1,1-dimethylurea (DCMU), an inhibitor of photosynthesis, and grown in the light.  
124 The four treatments provide conditions of no sugar/no light (Dark), sugar/no light (Suc),  
125 sugar/light (Light) and light/no sugar (DCMU) (Fig. 1A). We confirmed that seedling glucose  
126 content increased in the Suc and Light treatments but not in the Dark or DCMU treatments (Fig.  
127 1B). To capture both early and late transcriptional responses within the timeframe of a typical  
128 photoperiod, shoot tissue was harvested at subjective dawn (0 h) and 0.5, 2 and 8 h after the  
129 treatments and prepared for RNA-Seq.

130

131 We detected 5571 Suc-regulated genes that were differentially expressed between Dark and Suc  
132 treatments and 4628 DCMU-regulated genes differentially expressed between Light and DCMU  
133 (Fig. 1C, Dataset 1). The quantification of gene expression by RNA-seq was corroborated for 31  
134 representative transcripts by qRT-PCR with a strong positive correlation ( $R^2=0.91$ ) (Fig. S1). The  
135 overlap of differentially expressed genes (DEGs) between time-points was relatively low (Fig.  
136 1C), suggesting the sampling design captures a wide dynamic range of the transcriptional  
137 response. Comparison of our list of Suc-regulated genes to published microarray datasets (17,  
138 18) indicated that we have captured a more extensive sugar-regulated transcriptome (Fig. S2A).

139

140 To identify genes that are regulated by sugar, independent of light availability, we generated a list  
141 of genes that were upregulated by Suc in the dark and downregulated by DCMU in the light  
142 (sugar-activated; 927) or downregulated by Suc in the dark and upregulated by DCMU in the light  
143 (sugar-repressed; 1117) (Dataset 2; Fig. S3). The sugar-activated genes were enriched for Gene  
144 Ontology (GO) terms related to protein and cell wall synthesis (Fig. S3A). Sugar-repressed genes  
145 were enriched for GO terms related to light signalling, circadian rhythm and sugar metabolism  
146 (Fig. S3B, S3C). We compared our list of all 2042 sugar-regulated genes to published lists of  
147 genes regulated by SnRK1 and TOR, which are two major energy signalling hubs (2, 3). There  
148 was significant overlap with both datasets, but 1080 sugar-regulated genes were unique to this  
149 study (Fig. S3D), including 929 genes represented on ATH1 microarrays. These unique genes  
150 could represent responses either upstream or independent of SnRK1- and TOR-mediated  
151 signalling. Among the most significantly enriched GO terms in this list was Response to oxygen  
152 containing compound and Circadian rhythm (Fig. S3E).

153

154 To define the temporal characteristics of the complete transcriptome dataset, we performed  
155 clustering analysis of expression of 18071 genes across all 53 samples using variational  
156 Bayesian Gaussian mixture models (Fig. 1D, Dataset 3). We opted for 14 clusters as a tradeoff  
157 between maximizing the explained variance and producing meaningful clusters (Fig. S4, Fig. 1D).  
158 Several clusters were associated with either sugar-repressed (clusters 1-4) or sugar-activated  
159 (clusters 11-14) genes (Fig. 1D). We searched for enriched GO terms within each cluster  
160 (Dataset 3) and summarised these using an enrichment map of the top 15 terms within each  
161 cluster (Fig. 1E, Dataset 4). Some highly enriched GO term networks were specific to one or two  
162 clusters such as inositol phosphate processes in cluster 13 or circadian rhythm and growth in  
163 clusters 8 and 13. Other enrichment GO term networks represent four or five clusters. The largest  
164 of these networks included terms associated with metabolism of sugars, nucleotides and  
165 phospholipids, chloroplast function and proteostasis. The second largest enrichment network  
166 included terms associated with reactive oxygen species (ROS) metabolism and signalling,  
167 metabolic stress and immune responses.

168

169 Since GO terms associated with ROS appear to be a strong feature of the complete dataset, we  
170 hypothesised that ROS might be contributing to transcriptional responses to sugar. Indeed,  
171 Response to oxygen containing compound was the most significantly enriched GO term among  
172 all 2042 sugar-regulated genes and among Suc-regulated genes at 2 h (Fig. S2B). Within the  
173 former, 195 genes are associated with this GO term, including *ANNEXIN 2* (*ANN2*) and six  
174 *WRKY* transcription factor genes (Fig. 2A, Dataset 5). We also identified 95 sugar-regulated  
175 genes previously reported as ROS-responsive (19), including *ASCORBATE PEROXIDASE 1*  
176 (*APX1*) and *CATALASE 2* (*CAT2*) (Fig. 2B, Dataset 5).

177

178 To test whether treatment of Arabidopsis seedlings with sucrose affects production of ROS in  
179 dark-adapted seedlings, we used histochemical stains for hydrogen peroxide ( $H_2O_2$ ) and  
180 superoxide ( $O_2^-$ ) (Fig. 2C,D). Treatment of dark-adapted seedlings with sucrose led to a decrease  
181 in staining for  $H_2O_2$  within 30 min. By contrast, sucrose treatment of dark-adapted seedlings  
182 increased stain for  $O_2^-$  within 2 h, compared to mannitol controls. The elevated NBT stain was  
183 observed throughout the shoot, including hypocotyl, cotyledons and leaves. To corroborate this

184 observation, we used a L-012 luminescence assay, which does not discriminate between  $H_2O_2$   
185 and  $O_2^-$ , but provides better temporal resolution of ROS production than histochemical stains.  
186 Consistent with the NBT stains for  $O_2^-$ , we detected elevated L-012 luminescence within 2 h in  
187 sucrose-treated seedlings compared to mannitol-treated controls (Fig. 2E). Presumably, this  
188 assay underestimates the difference in  $O_2^-$  production since the signal in sucrose-treated  
189 seedlings will be the sum of the reduced  $H_2O_2$  and the increased  $O_2^-$  (Fig. 2C). The ROS-  
190 response detected in both the histochemical and luminescent assays is concomitant with the  
191 timing of the transcriptional response associated with ROS-related genes that we detected after 2  
192 h (Fig. 2A, 2B, S2B, Dataset 1).

193  
194 The accumulation of  $O_2^-$  in sucrose-treated seedlings might be a by-product of increased energy  
195 metabolism or could be contributing as a signal to affect transcriptional changes. We looked for  
196 chemicals that could inhibit the sucrose-induced production of  $O_2^-$ . Diphenyleiodonium (DPI) is  
197 an inhibitor of NADPH oxidases, which generate  $O_2^-$  at the plasma membrane. Methyl viologen  
198 (MV) interferes with electron transport from PS I and elevates  $O_2^-$ . 3-amino-1,2,4-triazole (3-AT)  
199 is a catalase inhibitor which promotes  $H_2O_2$  accumulation. We tested the effect of these  
200 chemicals on induction of a circadian-regulated luciferase reporter for *COLD*, *CIRCADIAN*  
201 *RHYTHM REGULATED 2* (*CCR2*). DPI strongly inhibited the increase of luciferase luminescence  
202 in sucrose-treated, dark-adapted *CCR2p:LUC* seedlings, whereas MV and 3-AT did not (Fig. 3A).  
203 Similarly, DPI, but not MV or 3-AT, also inhibited sucrose-induced L-012 luminescence (Fig. 3B)  
204 and histochemical staining for  $O_2^-$  but did not affect sucrose-induced changes in staining for  $H_2O_2$   
205 (Fig. 3C, D).

206  
207 We used the transcriptional response of *CCR2p:LUC* to generate a dose-response curve of  
208 inhibition by DPI. This response was inhibited by 30% at 1  $\mu$ M DPI and by >70% at  
209 concentrations above 5  $\mu$ M (Fig. 3E). Similar dose-dependent effects were also observed for two  
210 other NADPH oxidase inhibitors, VAS2870 (20) and apocynin (21), but not for the xanthine  
211 dehydrogenase inhibitor, allopurinol (22) (Fig S5). We confirmed that DPI also inhibited sucrose-  
212 induction of *CCR2* and *WRKY60* transcripts by qRT-PCR (Fig. 3F) as well as *WRKY11p: $\beta$ -*  
213 *GLUCURONIDASE* (*GUS*) and *WRKY30p: $\beta$ -GUS* reporters (Fig. S6). Thus, DPI effectively inhibits  
214 transcriptional regulation of multiple sugar-regulated genes.

215  
216 DPI could be inhibiting transcriptional responses to sugar in our assay by affecting uptake of  
217 sucrose, altered sugar metabolism, or inhibition of sugar sensing or signalling. We measured  
218 soluble sugars glucose, fructose and sucrose in sucrose-treated dark-adapted seedlings in the  
219 presence of DMSO or DPI. We did not detect a difference from controls for any sugar within 8 h  
220 of sucrose treatment (Fig. S7), suggesting that inhibition of sugar uptake or sucrose catabolism  
221 cannot account for the dramatic inhibition of the transcriptional response by DPI.

222  
223 Since DPI can inhibit transcriptional responses to sugar, we sought to establish whether DPI also  
224 affects other sugar-regulated processes in Arabidopsis. Seed germination in both dormant and  
225 non-dormant seeds is inhibited by exogenous sugar, acting through abscisic acid-dependent  
226 pathways (23). Similarly to sucrose, DPI also inhibits germination (24) (Fig. S8). If DPI inhibits  
227 germination by the same pathway as sucrose, we expected that their effects would be non-  
228 additive. However, the effect of DPI on inhibition of germination was detected both with and  
229 without sucrose in dormant and non-dormant seeds (Fig. S8). This suggests that DPI does not  
230 affect the regulatory pathways through which sucrose inhibits seed germination.

231  
232 Sugars promote growth. To test the effect of DPI on growth promotion by sucrose, we measured  
233 effects on hypocotyl elongation and root growth in dark-grown seedlings. This growth assay  
234 enables quantification of effects of sugar on cell elongation in the hypocotyl and cell division in  
235 the root in the absence of light signals. Seedlings growing on media containing DPI had slightly  
236 reduced hypocotyl length and root length in control media, and DPI strongly attenuated the

237 positive effects of sucrose on both hypocotyl and root length (Fig 3G). These data suggest that  
238 DPI inhibits the signalling or metabolism of sucrose to promote cell elongation and cell division.

239

240 NADPH oxidases are encoded by a family of ten *RESPIRATORY BURST OXIDASE HOMOLOG*  
241 (*RBOH*) genes in Arabidopsis. We tested whether *rboh* mutants had altered ROS production in  
242 dark-adapted seedlings using L-012 luminescence assays. Both the *rboh*b and *rboh*c mutants  
243 had similar response to sucrose as wild type, but *rboha* mutants and *rboh*d *rboh*f double mutants  
244 had reduced L-012 luminescence (Fig. S9A), similar to wild type treated with DPI, VAS2890 or  
245 apocynin (Fig. S5B). We also tested whether *rboh* mutants had altered growth responses to  
246 sucrose (Fig. S9B). The *rboh*d *rboh*f double mutant had reduced root and hypocotyl length on  
247 control media compared to wild type but growth was still responsive to sucrose in the mutant.  
248 Stimulation of hypocotyl growth by sucrose was reduced in the *rboha* mutant compared to wild  
249 type, but stimulation of root growth was unaffected. Thus, although we detected small growth  
250 effects in the mutants, none of those tested were able to phenocopy the effect of DPI. Similarly,  
251 the transcriptional response of *CCR2* or *WRKY60* to sucrose in dark adapted seedlings was not  
252 reduced in *rboh* mutants (Fig. S9C). These suggest that there is residual  $O_2^-$  accumulation in  
253 these mutants sufficient to elicit a response and that there is genetic redundancy in the molecular  
254 targets of DPI contributing to these sugar responses.

255

256 Sugars affect period of circadian rhythms (8) and the circadian clock contributes to rhythms of  
257 ROS homeostasis (13). We tested the effect of DPI, MV and 3-AT on circadian rhythms in media  
258 with or without sucrose. We measured circadian rhythms of *TOC1p:LUC* in continuous low light  
259 ( $10 \mu\text{mol m}^{-2} \text{s}^{-1}$ ) because the effect of exogenous sucrose on circadian rhythms is more  
260 pronounced in these conditions (8). Circadian period was significantly shorter in seedlings grown  
261 on sucrose compared to mannitol for all ROS modifiers, similar to the DMSO control (Fig. 4A,  
262 4B). This suggests that these chemicals did not affect the adjustment of period by exogenous  
263 sucrose.

264

265 Sugars also affect amplitude of circadian rhythms (11). Luciferase signal is dramatically elevated  
266 in *TOC1p:LUC* seedlings transferred to media containing sucrose compared to mannitol (Fig 4A,  
267 4C). This transcriptional response does not require *GI* (Fig. S10), a clock protein which is post-  
268 transcriptionally regulated by sucrose (11). The effect of sucrose in *TOC1p:LUC* seedlings was  
269 strongly attenuated in the presence of DPI, elevated in the presence of MV and unaffected by 3-  
270 AT (Fig. 4C), which is consistent with the effects of these compounds on  $O_2^-$  levels. The effects of  
271 DPI and MV were particularly pronounced during the night and were not observed in *CCA1p:LUC*  
272 or *PRR7p:LUC* seedlings (Fig. 4C), suggesting  $O_2^-$  acts on specific components of the oscillator.

273

274 Since the effects of DPI and MV differed between the morning-phased *CCA1p:LUC* and  
275 *PRR7p:LUC* and evening-phased *TOC1p:LUC*, we wondered whether this might reflect a global  
276 pattern of  $O_2^-$  on transcriptional rhythms. We used a set of previously reported  $O_2^-$ - and  $H_2O_2$ -  
277 responsive transcripts (19) to determine their phases in continuous light from a published RNA-  
278 seq dataset (25). The distribution of phases of transcripts up- and down-regulated by  $O_2^-$  or  $H_2O_2$   
279 deviated significantly from expectations (Fig. 4D, Dataset 5). The phase of transcripts  
280 upregulated by  $H_2O_2$  were enriched several hours after subjective dawn and downregulated  
281 transcripts were enriched before subjective dawn. This is consistent with the reported role of  
282 *CCA1* in driving rhythms of  $H_2O_2$  which peak in the early morning (13). By contrast, the phase of  
283 transcripts upregulated by  $O_2^-$ , which included *TOC1*, *GI*, *PRR5* and *LUX*, were enriched around  
284 subjective dusk. About 20% of these genes are direct *TOC1* targets (26) (Dataset 5). Transcripts  
285 down-regulated by  $O_2^-$ , including *LHY* and *RVE8*, were enriched around subjective dawn. This  
286 suggests that  $H_2O_2$  and  $O_2^-$  production or signalling are antiphased and is consistent with a role  
287 of  $O_2^-$  contributing to promoting oscillations of circadian transcripts in the evening.

288

289

290

291

292

## Discussion

293

294

295

296

297

298

299

300

301

302

303

304

305

306

307

308

309

310

311

312

We have identified ROS-regulated genes as a prominent feature in the response of the Arabidopsis transcriptome to sugars in both dark and light (Fig.1). The transcriptional response to sucrose in dark-adapted seedlings coincides with an increase in ROS levels, including  $O_2^-$  (Fig. 2). Both the accumulation of  $O_2^-$  and transcriptional response to sucrose were strongly attenuated in seedlings treated with DPI, a chemical inhibitor of flavoenzymes including NADPH oxidases (Fig. 3). DPI also inhibited the promotion of hypocotyl elongation and root growth by sucrose, demonstrating a broader impact of the ROS signal in sugar responses. Finally, we found that DPI inhibited the effect of sucrose on the evening expressed *TOC1* and identified a highly significant anti-phasing of rhythmic transcripts that are up- and down-regulated by  $O_2^-$  to dusk and dawn, respectively (Fig. 4). This is different to the redox effects of salicylic acid on both morning and evening genes (14). Thus, we propose that  $O_2^-$  functions as a metabolic signal associated with sugar levels which acts positively on the circadian oscillator in the evening. An association between cellular sugar status and redox state has been long recognised in the context of metabolism and oxidative stress (27), but our data provide evidence of a role for  $O_2^-$  as a dynamic sugar signal affecting daily rhythms of gene expression. This effect of sugar on the oscillator appears to be distinct from the T6P/SnRK1-mediated effect on period *via* transcriptional regulation of *PRR7* (7) (Fig. 4) and the post-transcriptional control of *GI* (11) (Fig. S9) revealing an additional layer of metabolic control of circadian rhythms in plants.

313

314

315

316

317

318

319

320

321

322

323

324

325

326

DPI is a potent inhibitor of NADPH oxidases which generate extracellular  $O_2^-$  at the plasma membrane activated by intracellular signals (28). We observed reduced sucrose-activated ROS production and modest growth phenotypes in *rboha* and *rboh* *rboh* mutants, but the transcriptional response to sucrose was similar to wild type (Fig. S8). Notwithstanding that the five *rboh* mutants examined here represent over 90% of total *RBOH* gene expression (Dataset 1), the subtle phenotypes in the *rboh* mutants compared to DPI-treated seedlings probably reflects functional redundancy within this gene family. This will be challenging to verify, since higher order mutants would be expected to be lethal. It is possible that effects of DPI on  $O_2^-$ -mediated responses to sugar can be attributed to inhibition of other flavoenzymes. For example, in photosynthetic organisms DPI inhibits  $O_2^-$  production from xanthine dehydrogenases, glutathione reductases and mitochondrial NAD(P)H dehydrogenases (29–31). However, the similar effects of VAS2890 and apocynin, but not allopurinol, on sugar responses support the role of NADPH oxidases (Fig. S5).

327

328

329

330

331

332

333

334

MV interferes with electron transport from PSI, as well as in mitochondria (32), and leads to accumulation of  $O_2^-$ , so the opposite effects on transcriptional responses might be expected compared to DPI. MV was unable to induce a transcriptional response in *CCR2p:LUC* seedlings without sucrose (Fig. 3A), which suggests that  $O_2^-$  alone does not activate circadian gene expression or that the site of  $O_2^-$  accumulation in MV-treated seedlings is not sufficient to act as the signal. However, MV elevated the response to sucrose in *TOC1p:LUC* seedlings (Fig. 4C) suggesting that  $O_2^-$  and sucrose might act synergistically.

335

336

337

338

339

340

341

342

343

$O_2^-$  is generated in mitochondria, chloroplasts, peroxisomes and the apoplast (28).  $O_2^-$  is typically scavenged quickly by superoxide dismutases. Elevation of  $O_2^-$  could be due to increased production or reduced scavenging. The increase in  $O_2^-$  triggered by sucrose in dark-adapted seedlings by histochemical stain and L-012 assay was relatively low and slow compared to elicitor-induced respiratory burst (33) but faster than a ROS effect reported for cell-wall damage (34). It might be that sucrose generates  $O_2^-$  in specific cell-types or subcellular locations and the signal might be diluted in bulk tissues or our detection methods might have insufficient sensitivity. This might explain why we couldn't detect L-012 luminescence in *rboh* *rboh* double mutants (Fig S8A). Thus, it will be useful to map the cellular and subcellular location of the  $O_2^-$  signal using the



344 expanding toolset of available redox probes (35–37). This will also provide clearer identity of  
345 candidate proteins producing the signal.

346  
347 Reversible oxidation of redox-sensitive proteins by ROS can alter their activity. In Arabidopsis,  
348 redox-sensitive proteins that are oxidised by H<sub>2</sub>O<sub>2</sub> have been identified in most cellular  
349 compartments (38). These include plasma membrane receptors (39), glycolytic enzymes (38, 40)  
350 which can localise in the nucleus and associate with DNA (41, 42) and transcription factors (43).  
351 Thus, localised changes in redox state could affect signalling pathways and gene expression by  
352 various mechanisms. Changes in localised O<sub>2</sub><sup>-</sup> concentration could modify protein function  
353 indirectly after dismutation to H<sub>2</sub>O<sub>2</sub>, or directly by affecting Fe-S proteins (28).

354  
355 It is experimentally difficult to separate the effects of H<sub>2</sub>O<sub>2</sub>, O<sub>2</sub><sup>-</sup> or other ROS on protein oxidation.  
356 Differences in target specificity for ROS might depend on their redox dynamics or subcellular  
357 location. H<sub>2</sub>O<sub>2</sub> is regarded as the most likely ROS signal because it is relatively stable compared  
358 to the more reactive O<sub>2</sub><sup>-</sup> (28). However, our phase analyses of H<sub>2</sub>O<sub>2</sub> and O<sub>2</sub><sup>-</sup> regulated transcripts  
359 indicates clear temporal separation of their effects (Fig. 4). This might reflect differences in spatial  
360 organisation of oxidative metabolism at different times of day. The mechanism by which sugar-  
361 activated O<sub>2</sub><sup>-</sup> production affects gene regulation will depend on its cellular location.

362  
363 By examining the effects of sugar on the Arabidopsis transcriptome independently of light, we  
364 have uncovered a role for redox status, exemplified by accumulation of O<sub>2</sub><sup>-</sup>, that promotes  
365 responses to sugar including growth and circadian rhythms. In contrast to the previously reported  
366 association of circadian rhythms of H<sub>2</sub>O<sub>2</sub>, which are phased in the morning (13), the O<sub>2</sub><sup>-</sup>-activated  
367 transcriptome peaks in the evening and includes core genes within the circadian oscillator. Sugar  
368 promotes O<sub>2</sub><sup>-</sup> which alters gene expression by either an extracellular or intracellular redox signal  
369 which could transmit to the nucleus via signalling or protein localisation. We propose that this  
370 metabolic signal functions to coordinate rhythmic physiology and growth in response to  
371 environmental conditions that affect photosynthetic metabolism.

372

## 373 **Materials and Methods**

374

375 Details of plant materials and growth conditions, RNA-Seq and clustering, qRT-PCR,  
376 histochemical stains, luminescence assays and sugar quantification are described in SI  
377 Appendix. Primers are listed in Dataset 6.

378

## 379 **Acknowledgments**

380

381 We thank Ms. Heather Eastmond (University of York) for technical support and Prof Alex Webb  
382 (University of Cambridge) for useful comments on the manuscript. This research was funded by  
383 BBSRC grant (BB/L021188/1) to MJH and IAG, Royal Society Research Grant (RG150144) to  
384 MJH and by The University of Melbourne through the Research Grants Support Scheme to MJH  
385 and a Melbourne Research Scholarship to XL. This research was not funded by the Australian  
386 Research Council.

387

## 388 **References**

389

- 390 1. H. A. Herrmann, J. M. Schwartz, G. N. Johnson, Metabolic acclimation - A key to  
391 enhancing photosynthesis in changing environments? *J. Exp. Bot.* **70**, 3043–3056 (2019).
- 392 2. E. Baena-González, F. Rolland, J. M. Thevelein, J. Sheen, A central integrator of  
393 transcription networks in plant stress and energy signalling. *Nature* **448**, 938–42 (2007).
- 394 3. Y. Xiong, *et al.*, Glucose-TOR signalling reprograms the transcriptome and activates  
395 meristems. *Nature* **496**, 181–6 (2013).

- 396 4. H. Schlupepmann, T. Pellny, A. van Dijken, S. Smeekens, M. Paul, Trehalose 6-phosphate  
397 is indispensable for carbohydrate utilization and growth in *Arabidopsis thaliana*. *Proc. Natl.*  
398 *Acad. Sci. U. S. A.* **100**, 6849–6854 (2003).
- 399 5. C. Nunes, *et al.*, The Trehalose-6-phosphate / SnRK1 signaling pathway primes growth  
400 recovery following relief of sink limitation. *Plant Physiology* **162**, 1720–1732 (2013).
- 401 6. M. J. Haydon, X. Li, M. K. Y. Ting, Temporal control of plant-environment interactions by  
402 the circadian clock. *Annu. Plant Rev. online* **2**, 1–32 (2019).
- 403 7. A. Frank, *et al.*, Circadian Entrainment in *Arabidopsis* by the Sugar-Responsive  
404 Transcription Factor bZIP63. *Curr. Biol.* **28**, 2597-2606.e6 (2018).
- 405 8. M. J. Haydon, O. Mielczarek, F. C. Robertson, K. E. Hubbard, A. a. R. Webb,  
406 Photosynthetic entrainment of the *Arabidopsis* circadian clock. *Nature* **502**, 689–692  
407 (2013).
- 408 9. J. Shin, *et al.*, The metabolic sensor AKIN10 modulates the *Arabidopsis* circadian clock in  
409 a light-dependent manner. *Plant Cell Environ.* **40**, 997–1008 (2017).
- 410 10. N. Zhang, *et al.*, Metabolite-mediated TOR signaling regulates the circadian clock in  
411 *Arabidopsis*. *Proc. Natl. Acad. Sci. U. S. A.* **116**, 25395–25397 (2019).
- 412 11. M. J. Haydon, O. Mielczarek, A. Frank, Á. Román, A. A. R. Webb, Sucrose and ethylene  
413 signaling interact to modulate the circadian clock. *Plant Physiol.* **175**, pp.00592.2017  
414 (2017).
- 415 12. N. Dalchau, *et al.*, The circadian oscillator gene GIGANTEA mediates a long-term  
416 response of the *Arabidopsis thaliana* circadian clock to sucrose. *Proc. Natl. Acad. Sci. U.*  
417 *S. A.* **108**, 5104–5109 (2011).
- 418 13. A. G. Lai, *et al.*, CIRCADIAN CLOCK-ASSOCIATED 1 regulates ROS homeostasis and  
419 oxidative stress responses. *Proc. Natl. Acad. Sci.* **109**, 17129–17134 (2012).
- 420 14. M. Zhou, *et al.*, Redox rhythm reinforces the circadian clock to gate immune response.  
421 *Nature* **523**, 472–476 (2015).
- 422 15. R. Edgar, *et al.*, Peroxiredoxins are conserved markers of circadian rhythms. *Nature* **485**,  
423 459–464 (2012).
- 424 16. E. Shor, I. Paik, S. Kangisser, R. Green, E. Huq, PHYTOCHROME INTERACTING  
425 FACTORS mediate metabolic control of the circadian system in *Arabidopsis*. *New Phytol.*  
426 **215**, 217–228 (2017).
- 427 17. K. E. Thum, M. J. Shin, P. M. Palenchar, A. Kouranov, G. M. Coruzzi, Genome-wide  
428 investigation of light and carbon signaling interactions in *Arabidopsis*. *Genome Biol.* **5**,  
429 R10 (2004).
- 430 18. D. Osuna, *et al.*, Temporal responses of transcripts , enzyme activities and metabolites  
431 after adding sucrose to carbon-deprived *Arabidopsis* seedlings. *Plant J.* **49**, 463–491  
432 (2007).
- 433 19. I. Gadjev, *et al.*, Transcriptomic footprints disclose specificity of reactive oxygen species  
434 signaling in *Arabidopsis*. *Plant Physiol.* **141**, 436–445 (2006).
- 435 20. S. Mangano, *et al.*, Molecular link between auxin and ROS-mediated polar growth. *Proc.*

- 436 *Natl. Acad. Sci. U. S. A.* **114**, 5289–5294 (2017).
- 437 21. J. Stolk, T. J. Hiltermann, J. H. Dijkman, A. J. Verhoeven, Characteristics of the inhibition  
438 of NADPH oxidase activation in neutrophils by apocynin, a methoxy-substituted catechol.  
439 *Am. J. Respir. Cell Mol. Biol.* **11**, 95–102 (1994).
- 440 22. C. Hesberg, R. Hänsch, R. R. Mendel, F. Bittner, Tandem orientation of duplicated  
441 xanthine dehydrogenase genes from *Arabidopsis thaliana*: Differential gene expression  
442 and enzyme activities. *J. Biol. Chem.* **279**, 13547–13554 (2004).
- 443 23. J. Price, T. C. Li, S. G. Kang, J. K. Na, J. C. Jang, Mechanisms of glucose signaling  
444 during germination of *Arabidopsis*. *Plant Physiol.* **132**, 1424–1438 (2003).
- 445 24. K. Müller, A. C. Carstens, A. Linkies, M. A. Torres, G. Leubner-metzger, The NADPH-  
446 oxidase AtrbohB plays a role in *Arabidopsis* seed after-ripening. *New Phytol.* **184**, 885–  
447 897 (2009).
- 448 25. A. Romanowski, R. G. Schlaen, S. Perez-Santangelo, E. Mancini, M. J. Yanovsky, Global  
449 transcriptome analysis reveals circadian control of splicing events in *Arabidopsis thaliana*.  
450 *Plant J.* **103**, 889–902 (2020).
- 451 26. W. Huang, *et al.*, Mapping the core of the *Arabidopsis* circadian clock defines the network  
452 structure of the oscillator. *Science (80-. )*. **336**, 75–79 (2012).
- 453 27. I. Couée, C. Sulmon, G. Gouesbet, A. El Amrani, Involvement of soluble sugars in reactive  
454 oxygen species balance and responses to oxidative stress in plants. *J. Exp. Bot.* **57**, 449–  
455 459 (2006).
- 456 28. N. Smirnov, D. Arnaud, Hydrogen peroxide metabolism and functions in plants. *New*  
457 *Phytol.* **221**, 1197–1214 (2019).
- 458 29. M. Zarepour, *et al.*, Xanthine dehydrogenase AtXDH1 from *Arabidopsis thaliana* is a  
459 potent producer of superoxide anions via its NADH oxidase activity. *Plant Mol. Biol.* **72**,  
460 301–310 (2010).
- 461 30. J. M. Diaz, *et al.*, NADPH-dependent extracellular superoxide production is vital to  
462 photophysiology in the marine diatom *Thalassiosira oceanica*. *Proc. Natl. Acad. Sci. U. S.*  
463 *A.* **116**, 16448–16453 (2019).
- 464 31. T. H. Roberts, K. M. Fredlund, I. M. Møller, Direct evidence for the presence of two  
465 external NAD(P)H dehydrogenases coupled to the electron transport chain in plant  
466 mitochondria. *FEBS Lett.* **373**, 307–309 (1995).
- 467 32. F. Cui, *et al.*, Interaction of methyl viologen-induced chloroplast and mitochondrial  
468 signalling in *Arabidopsis*. *Free Radic. Biol. Med.* **134**, 555–566 (2019).
- 469 33. J. M. Smith, A. Heese, Rapid bioassay to measure early reactive oxygen species  
470 production in *Arabidopsis* leaf tissue in response to living *Pseudomonas syringae*. *Plan*  
471 *Methods* **10**, 6 (2014).
- 472 34. L. Denness, *et al.*, Cell Wall Damage-Induced Lignin Biosynthesis Is Regulated by a  
473 Reactive Oxygen Species- and Jasmonic Acid-dependent Process in *Arabidopsis*. *Plant*  
474 *Physiol.* **156**, 1364–1374 (2011).
- 475 35. A. J. Meyer, *et al.*, Redox-sensitive GFP in *Arabidopsis thaliana* is a quantitative biosensor  
476 for the redox potential of the cellular glutathione redox buffer. *Plant J.* **52**, 973–986 (2007).

- 477 36. T. Nietzel, *et al.*, The fluorescent protein sensor rGFP2-Orp1 monitors in vivo H<sub>2</sub>O<sub>2</sub>  
478 and thiol redox integration and elucidates intracellular H<sub>2</sub>O<sub>2</sub> dynamics during elicitor-  
479 induced oxidative burst in Arabidopsis. *New Phytol.* **221**, 1649–1664 (2019).
- 480 37. J. Steinbeck, *et al.*, In vivo NADH/NAD<sup>+</sup> biosensing reveals the dynamics of cytosolic  
481 redox metabolism in plants. *Plant Cell* **32**, 3324–3345 (2020).
- 482 38. P. Liu, H. Zhang, H. Wang, Y. Xia, Identification of redox-sensitive cysteines in the  
483 arabidopsis proteome using OxiTRAQ, a quantitative redox proteomics method.  
484 *Proteomics* **14**, 750–762 (2014).
- 485 39. F. Wu, *et al.*, Hydrogen peroxide sensor HPCA1 is an LRR receptor kinase in Arabidopsis.  
486 *Nature* **578**, 577–581 (2020).
- 487 40. C. H. Marchand, *et al.*, Thioredoxin targets in Arabidopsis roots. *Proteomics* **10**, 2418–  
488 2428 (2010).
- 489 41. Y. H. Cho, S. D. Yoo, J. Sheen, Regulatory Functions of Nuclear Hexokinase1 Complex in  
490 Glucose Signaling. *Cell* **127**, 579–589 (2006).
- 491 42. S. C. Kim, L. Guo, X. Wang, Nuclear moonlighting of cytosolic glyceraldehyde-3-  
492 phosphate dehydrogenase regulates Arabidopsis response to heat stress. *Nat. Commun.*  
493 **11**, 1–15 (2020).
- 494 43. Y. Li, W. Liu, H. Zhong, H. L. Zhang, Y. Xia, Redox-sensitive bZIP68 plays a role in  
495 balancing stress tolerance with growth in Arabidopsis. *Plant J.* **100**, 768–783 (2019).

496

497

498

## 499 Figures legends

500

501 **Figure 1.** A light-independent sugar-regulated transcriptome of Arabidopsis. (A) Two week old  
502 seedlings were grown in the dark for 72 h, then transferred to 10 mM mannitol (Dark) or sucrose  
503 (Suc) in the dark, or into the light with 10 mM mannitol (Light) or 20 μM DCMU and 10 mM  
504 mannitol (DCMU). Shoot tissue was collected at 0, 0.5, 2 and 8 h for RNA-Seq. (B) Leaf glucose  
505 content in seedlings grown as in (A) (means ± SD, N = 3; \* P < 0.05 from Dark; Bonferroni-  
506 corrected t-test). (C) Venn diagrams of differentially expressed genes at each time-point in  
507 samples collected in the dark (left) or light (right). (D) Expression trajectories of 14 clusters of co-  
508 expressed genes identified by variational Bayesian Gaussian mixture model. Pink and blue lines  
509 indicate genes identified as up/down or down/up regulated by sucrose/DCMU, respectively. The  
510 number of genes within each cluster are in parentheses. (E) Gene Ontology enrichment maps of  
511 the top 15 terms in each cluster in (D). Node colours correspond to the cluster(s) represented in  
512 (D). Node sizes are proportional to the number of genes. Selected nodes are labelled with  
513 significantly enriched, representative GO terms for each network. See Dataset 4 for the fully  
514 annotated networks.

515

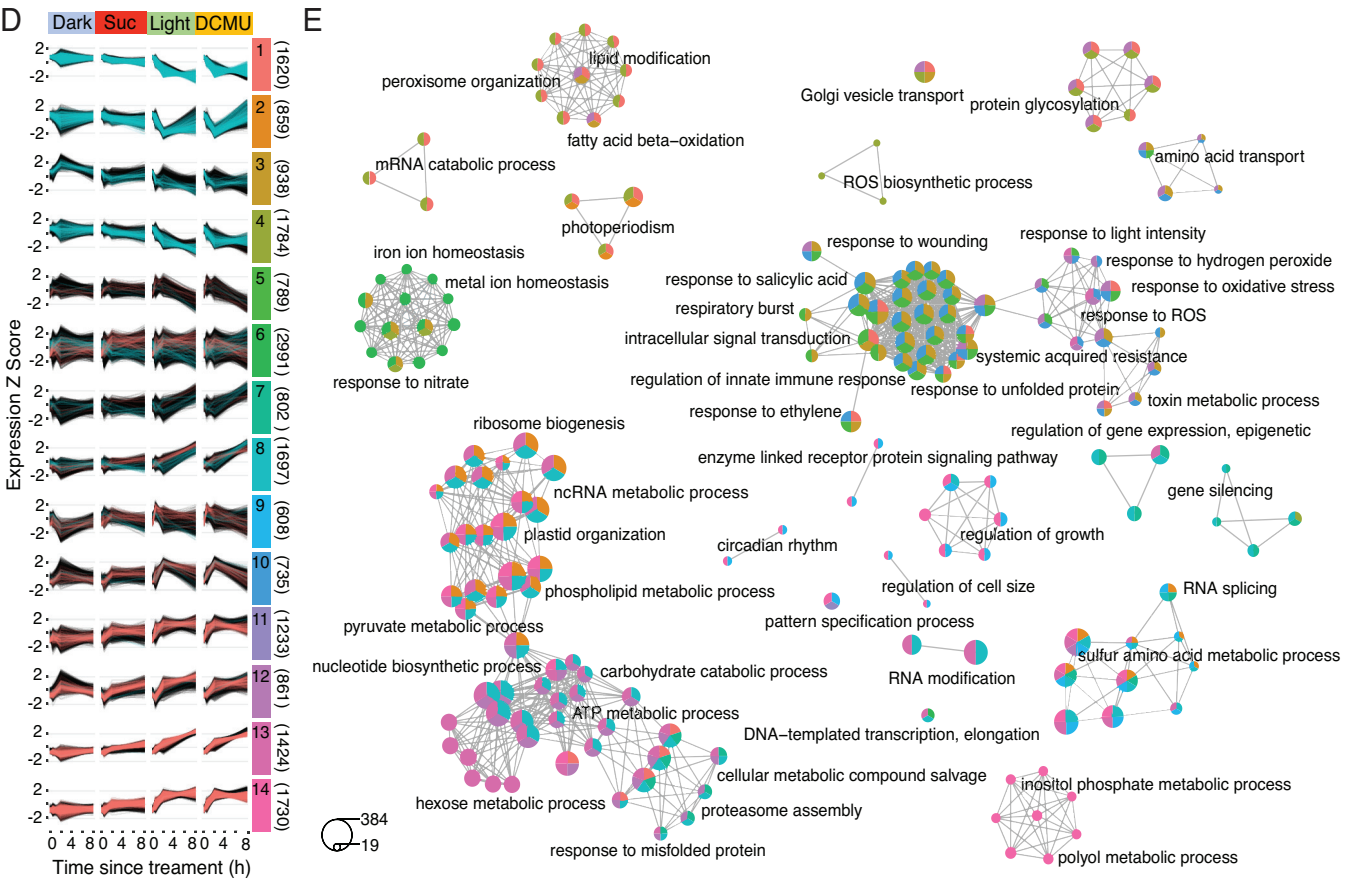
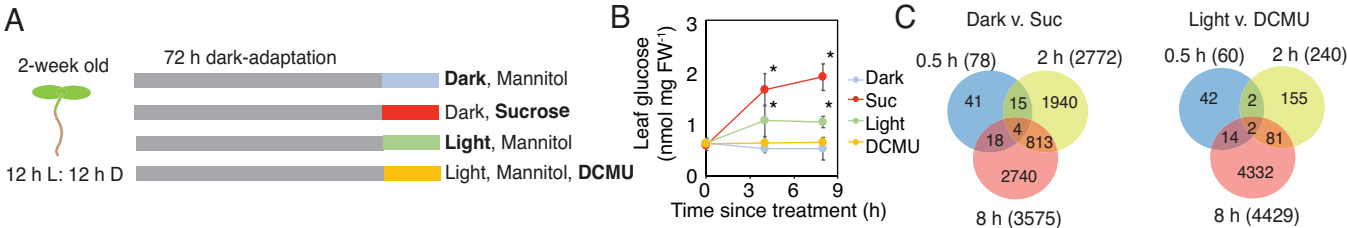
516 **Figure 2.** Sucrose promotes superoxide production and ROS-regulated transcripts in dark-  
517 adapted seedlings. Transcript levels of representative ROS-associated genes identified as sugar-  
518 regulated from RNA-seq that are (A) from the GO class ‘responsive to oxygen-containing  
519 compound’ or (B) identified from a previous study (19) (means ± SD, N = 3). (C) Histochemical  
520 stains for hydrogen peroxide (DAB) and superoxide (NBT) in 10 d old, dark-adapted Col-0  
521 seedlings treated with 30 mM mannitol or sucrose. (D) DAB and NBT stain intensity in seedlings  
522 grown as in (C) (means ± SD, N = 6; P < 0.05 from mannitol; Bonferroni-corrected t-test). (E) L-

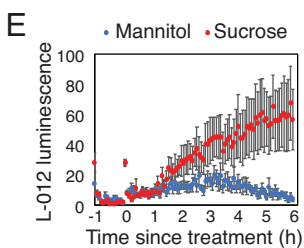
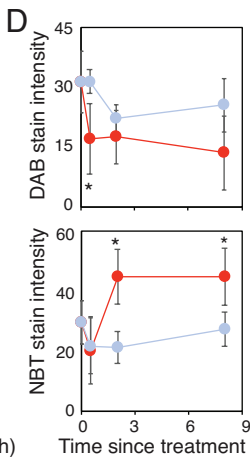
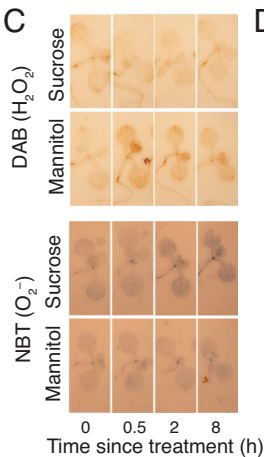
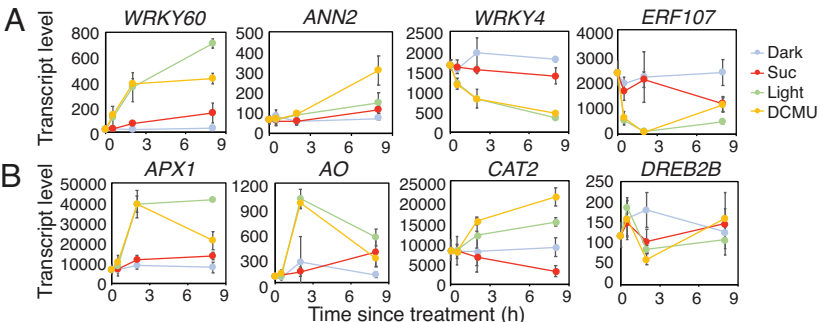
523 012 luminescence in dark-adapted Col-0 treated with 30 mM mannitol or sucrose (means  $\pm$  SEM,  
524  $N = 6$ ).

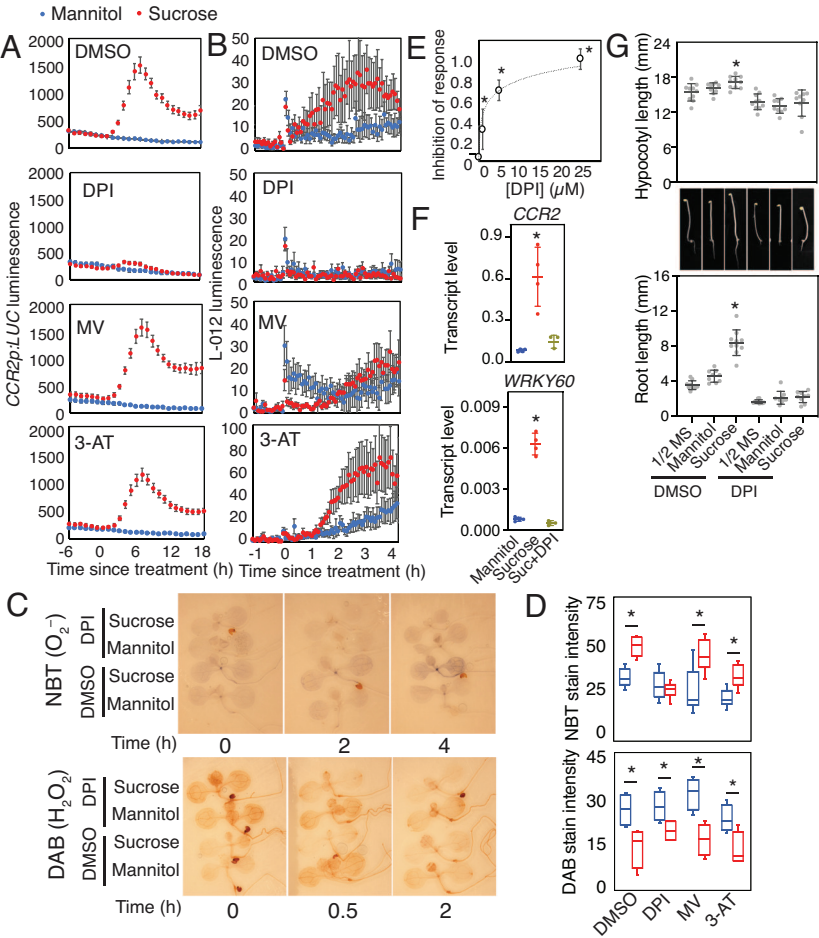
525 **Figure 3.** Modifiers of superoxide inhibit responses to sucrose. (A) Luciferase luminescence in  
526 dark-adapted *CCR2p:LUC* seedlings treated with 30 mM mannitol or sucrose in the presence of  
527 DMSO, 10  $\mu$ M DPI, 2  $\mu$ M MV or 200  $\mu$ M 3-AT (means  $\pm$  SEM,  $N = 6$ ). (B) L-012 luminescence in  
528 dark-adapted Col-0 treated as in (A) (means  $\pm$  SEM,  $N = 6$ ). (C) Histochemical NBT stain for  $O_2^-$   
529 and DAB stains for  $H_2O_2$  in dark-adapted Col-0 seedlings treated with 30 mM mannitol or sucrose  
530 in the presence of 0.1% DMSO or 10  $\mu$ M DPI. (D) Stain intensity in Col-0 seedlings 4 h (NBT) or  
531 0.5 h (DAB) after treatment as in (A) ( $N = 6$ ; \*  $P < 0.05$ ;  $t$ -test). (E) Inhibition of response of  
532 luciferase luminescence to 30 mM sucrose in dark-adapted *CCR2p:LUC* seedlings in the  
533 presence of 0 (0.1% DMSO), 1, 5 or 25  $\mu$ M DPI. (means  $\pm$  SEM,  $N = 3$ ; \*  $P < 0.05$  from DMSO;  
534 Bonferroni-corrected  $t$ -test). (F) Transcript level of *CCR2* and *WRKY60*, relative to *UBQ10* in  
535 dark-adapted Col-0 seedlings 8 h after treatment with 30 mM mannitol, sucrose or sucrose with  
536 10  $\mu$ M DPI (means  $\pm$  SD,  $N = 4$ ; \*  $P < 0.05$  from mannitol; Bonferroni-corrected  $t$ -test. (G)  
537 Hypocotyl length and root length of 5 d old dark-grown Col-0 seedlings grown on  $\frac{1}{2}$  MS with or  
538 without 30 mM mannitol or sucrose, 0.1% DMSO or 1  $\mu$ M DPI (means  $\pm$  SD,  $N = 10$ ; \*  $P < 0.05$   
539 from  $\frac{1}{2}$  MS; Bonferroni-corrected  $t$ -test).

540 **Figure 4.** Modifiers of superoxide affect modulation of circadian rhythms by sucrose. (A)  
541 Normalised luciferase luminescence in *TOC1p:LUC* seedlings in continuous low light with 30 mM  
542 mannitol (blue) or sucrose (red) in the presence of 0.1% DMSO or 10  $\mu$ M DPI, 2  $\mu$ M MV or 200  
543  $\mu$ M 3-AT (means  $\pm$  SD,  $N = 4$ ). (B) Circadian period estimates of luciferase luminescence in  
544 *TOC1p:LUC* seedlings in (A) (means  $\pm$  SD,  $N = 4$ ; \*  $P < 0.05$  from mannitol; Bonferroni-corrected  
545  $t$ -test). (C) Luciferase luminescence in *TOC1p:LUC*, *PRR7p:LUC* and *CCA1p:LUC* seedlings for  
546 24 h in light/dark treated as in (A) (means  $\pm$  SD,  $N = 4$ ). (D) Phase of rhythmic  $O_2^-$ - and  $H_2O_2^-$ -  
547 responsive transcripts in continuous light. Values are enrichment (observed/expected) of up- and  
548 down-regulated genes in each 4-h phase window (\*  $P < 0.01$ ;  $\chi^2$ ).

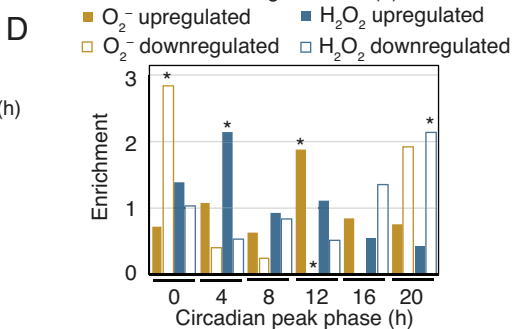
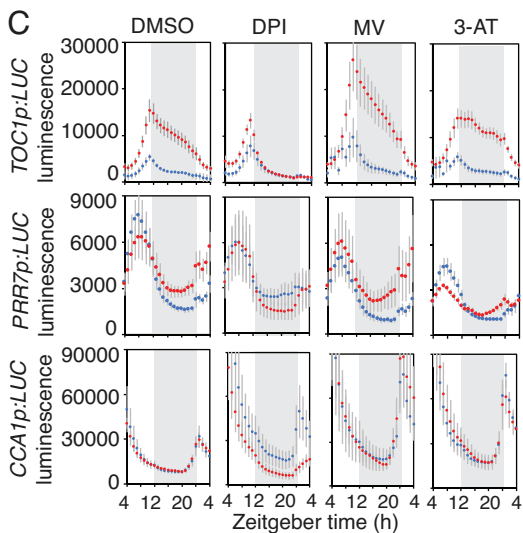
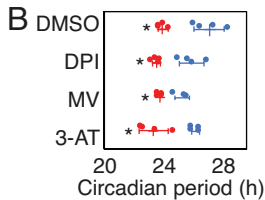
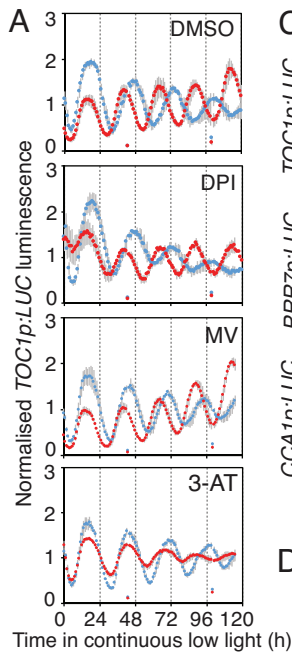
549











# PNAS

www.pnas.org

1  
2  
3  
4  
5  
6  
7  
8  
9  
10  
11  
12  
13  
14  
15  
16  
17  
18  
19  
20  
21  
22  
23  
24  
25  
26  
27  
28  
29  
30  
31  
32  
33  
34  
35

Supplementary Information for

Superoxide is promoted by sucrose and affects amplitude of circadian rhythms in the evening

Ángela Román, Xiang Li, Dongjing Deng, John W. Davey, Sally James, Ian A Graham, Michael J Haydon

Michael J. Haydon  
Email: m.haydon@unimelb.edu.au

**This PDF file includes:**

Supplementary text  
Figures S1 to S10  
Legends for Datasets 1 to 6  
SI References

**Other supplementary materials for this manuscript include the following:**

Datasets 1 to 6

36

## 37 Supplementary Information Text

### 38 Materials and Methods

39 **Plant materials and growth conditions.** Col-0 was used as wild-type *Arabidopsis thaliana*.  
40 *CCR2p:LUC*, *CCA1p:LUC*, *PRR7p:LUC* and *TOC1p:LUC* transgenic lines have been described  
41 previously (1). Mutants *rboha*, *rbohbc*, *rbohbc/root hair defective2-1* and *rbohhd rbohfc* and  
42 *WRKY11p:GUS* and *WRKY30p:GUS* transgenic lines were obtained from Arabidopsis Biological  
43 Resource Centre (ABRC). Mutant *tps1-12* (2) was backcrossed twice to Col-0.

44

45 Seeds were surface sterilised with 30% (v/v) bleach, 0.02% (v/v) Triton X-100, washed three  
46 times with sterile deionised water and sown on ½ strength Murashige & Skoog (½ MS), pH 5.7 or  
47 modified Hoagland media, pH 5.7 (3) solidified with 0.8% (w/v) agar Type M (Sigma). After 2 d in  
48 the dark at 4°C, seedlings were grown at 20°C in 12 h light/12 dark cycles (LD) under 100-140  
49  $\mu\text{mol m}^{-2} \text{s}^{-1}$  light. Concentrations of DPI, MV and 3-AT were based on a previous study (4)

50

51 For dark growth assays, seeds were germinated on ½ MS in LD for 48 h. Within 1 h of dawn  
52 before photomorphogenesis, germinated seeds were transferred to ½ MS with 1% (w/v) agar  
53 containing treatments, wrapped in foil and grown vertically for 3 d. Plates were photographed and  
54 root and hypocotyl lengths were quantified with ImageJ (NIH).

55

56 **RNA-seq.** Col-0 seeds were sown on nylon membrane on modified Hoagland's solution and  
57 grown at 45° angle. Two week old seedlings were wrapped in aluminium foil before dawn and  
58 grown in the dark for 72 h. Under dim green light, dark-adapted seedlings were transferred to  
59 Hoagland's media containing 10 mM mannitol or 10 mM sucrose and maintained in the dark or 10  
60 mM mannitol with or without 20  $\mu\text{M}$  DCMU and returned to the light. Shoots of 40 seedlings were  
61 collected at 0, 0.5, 2 and 8 h after treatments, snap-frozen in liquid nitrogen and stored at -80°C  
62 until processing. The RNA-seq samples were taken from two independent experiments; the first  
63 produced three biological replicates for all conditions, and the second, three further replicates for  
64 the dark-grown 0, 2 and 8 h conditions. RNA was extracted with RNeasy Plant Mini Kit including  
65 on-column DNase treatment (Qiagen). RNA quantity and purity were confirmed using a  
66 Nanodrop spectrophotometer (ThermoScientific), and samples were run on an Agilent 2100  
67 Bioanalyzer, with RNA 6000 Nano kit, to confirm RNA integrity (all samples displayed RINs of >  
68 7). mRNA sequencing libraries were prepared from 1  $\mu\text{g}$  total RNA using the NEBNext RNA Ultra  
69 Directional Library preparation kit for Illumina (New England BioLabs Inc.), in conjunction with the  
70 NEBNext Poly(A) mRNA Magnetic Isolation Module and NEBNext multiplex oligos for Illumina  
71 (dual 8 bp indexing primers set 1), according to the manufacturer's instructions. Libraries were  
72 pooled at equimolar ratios, and the pool was sent for 2 x 150 base paired end sequencing on a  
73 HiSeq 3000 at the University of Leeds Next Generation Sequencing Facility. Each sample was  
74 sequenced twice on two separate lanes, except replicate 3 of the light 2 h condition, which failed  
75 and was resequenced on one lane only, and replicate 1 of the 0 h condition in experiment 2,  
76 which also failed and was not resequenced. Raw reads have been uploaded to the European  
77 Nucleotide Archive, ENA accession PRJEB40453 [these will be made public on acceptance].

78

79 RNA-seq samples were quantified with Salmon v0.8.2 (5) using options -l ISR, --seqBias, --  
80 gcBias, --useVBOpt and --numBootstraps 30 and providing both lanes of sequencing for each  
81 sample as input. The reference was Araport11 files Araport11\_genes.201606.cdna.fasta.gz and  
82 Araport11\_GFF3\_genes\_transposons.201606.gtf.gz, downloaded from  
83 [https://www.arabidopsis.org/download/index-](https://www.arabidopsis.org/download/index-auto.jsp?dir=%2Fdownload_files%2FGenes%2FAraport11_genome_release)  
84 [auto.jsp?dir=%2Fdownload\\_files%2FGenes%2FAraport11\\_genome\\_release](https://www.arabidopsis.org/download/index-auto.jsp?dir=%2Fdownload_files%2FGenes%2FAraport11_genome_release) on 26 April 2017  
85 (included in Dryad repository []). A map of transcript names to gene names to use with Salmon  
86 option -g was created with the following Unix one liner:

87

```
88 cut -f9 Araport11_GFF3_genes_transposons.201606.gtf | sort | uniq |  
89 perl -ne 'print "\$1\t\$2\n" if /transcript_id "(.+)"; gene_id "(.+)";/'  
> Araport11_GFF3_gene_transposons.201606.salmon.geneMap.tsv
```

90 Salmon output was converted to sleuth-compatible format with wasabi  
91 (<https://github.com/COMBINE-lab/wasabi>, commit f31c73e). These files will be included in a  
92 Dryad repository (<https://datadryad.org>) on acceptance but can be accessed during peer review  
93 here <https://drive.google.com/drive/folders/18zc1PCFyZaRTnxTce3lVdhwPFZ11inCm/>.  
94  
95

96 Differential expression was analysed with Sleuth v0.29.0 (6) with multiple testing correction by  
97 stageR v0.1.0, commit 59af4d7 (7), against the Araport11 gene annotation (8) imported from  
98 Ensembl Genomes release 36 (9) with biomaRt (10). Models were run with a log<sub>2</sub> transformation  
99 function on the counts (log<sub>2</sub>(x+0.5)). A Sleuth model was built for each pairwise comparison  
100 (Dark vs Sucrose 0.5 h, Dark vs Sucrose 2 h, Dark vs Sucrose 8 h, Light vs DCMU 0.5 h, Light vs  
101 DCMU 2 h, Light vs DCMU 8 h) with differentially expressed genes detected with a Wald test for  
102 each comparison. A full model was run on all samples including control 0 h samples with  
103 differentially expressed genes detected with a likelihood ratio test. Screening p-values for stageR  
104 were taken from the full model's likelihood ratio test and confirmation p-values from the pairwise  
105 models' Wald tests. stageR results targeted a 10% overall false discovery rate using the Holm  
106 method for family-wise error rate correction. R code to run Sleuth and stageR analyses is  
107 provided in our Dryad repository (run\_sleuth.R, run\_stageR.R). Comparisons between gene lists  
108 were made using a Venn diagram tool <http://bioinformatics.psb.ugent.be/webtools/Venn/>. Gene  
109 ontology (GO) enrichment of these lists used PANTHER Classification System (11) accessed  
110 through The Arabidopsis Information Resource (TAIR).  
111

112 **qRT-PCR.** cDNA was prepared from 0.5 µg RNA in 10 µl reactions using Tetro cDNA synthesis  
113 kit (Bioline). 0.5 ng/µl of cDNA was used in each PCR reaction with 0.2 µM primers in the  
114 SensiFAST SYBR no-ROX kit (Bioline) on a CFX96 Touch Real-time PCR detection system (Bio-  
115 Rad). PCR reaction efficiencies were determined for each primer pair using LinRegPCR (12) and  
116 transcript levels were determined for target and reference genes using (mean PCR efficiency)<sup>-Ct</sup>.  
117 Primer sequences are listed in Dataset 5.  
118

119 **Transcriptome Clustering.** Genes were clustered based on Sleuth scaled\_reads\_per\_base  
120 abundance values for each sample, using scikit-learn's BayesianGaussianMixture (13)  
121 <https://scikit-learn.org/stable/modules/generated/sklearn.mixture.BayesianGaussianMixture.html>)  
122 with maximum 1000 iterations. Numbers of clusters from 2 to 20 were tested, with the 14 cluster  
123 output chosen for further analysis. Gene Ontology Enrichment analysis for each cluster was  
124 performed with R's clusterProfiler (14)  
125 [https://bioconductor.org/packages/release/bioc/vignettes/clusterProfiler/inst/doc/clusterProfiler.ht](https://bioconductor.org/packages/release/bioc/vignettes/clusterProfiler/inst/doc/clusterProfiler.html)  
126 [ml](https://bioconductor.org/packages/release/bioc/vignettes/clusterProfiler/inst/doc/clusterProfiler.html)). R code for clustering is provided in the Dryad repository (cluster\_analysis.R).  
127

128 **Histochemical stains.** Seeds were sown on ½ MS and grown in LD and 11 d old seedlings were  
129 wrapped in aluminium foil at dusk. After 72 h, at subjective dusk under dim green light, seedlings  
130 were transferred into 0.5 ml liquid ½ MS containing 0.1% (v/v) DMSO or chemical treatments in  
131 48-well plates. At the following subjective dawn in dim green light, 0.5 ml of 60 mM mannitol or  
132 sucrose was added (30 mM final sugar concentration). For H<sub>2</sub>O<sub>2</sub> stains, 1 mg/ml (w/v) 3'-  
133 diaminobenzidine tetrahydrochloride hydrate was dissolved in 50 mM Tris acetate (pH 5.0). For  
134 O<sub>2</sub><sup>-</sup> stains, 2 mg/ml (w/v) nitroblue tetrazolium was dissolved in 10 mM potassium phosphate  
135 buffer (pH 7.8), 10 mM NaN<sub>3</sub>. Seedlings were vacuum infiltrated for 1 min in freshly prepared  
136 staining solutions and incubated in the dark for 24 h. Samples were cleared by boiling for 5 min in  
137 1:1:4 lactic acid:glycerol:ethanol then transferred to 1:4 glycerol:ethanol. GUS-stains of  
138 transgenic lines was performed overnight as previously (15). Stained seedlings were mounted  
139 under coverslips on microscope slides and imaged immediately with a SMZ800 stereomicroscope  
140 (Nikon) or a V370 Photo flatbed scanner (Epson). DAB and NBT stain intensity were quantified in  
141 whole shoots by dividing integrated density by area of individual seedlings and subtracting  
142 background signal in ImageJ (NIH).  
143

144 **L-012 luminescence assay.** Clusters of 7 d old seedlings grown on ½ MS or 6 mm leaf discs  
145 from 4 week old plants grown in LD were transferred to 96-well luminescence plates (Greiner)

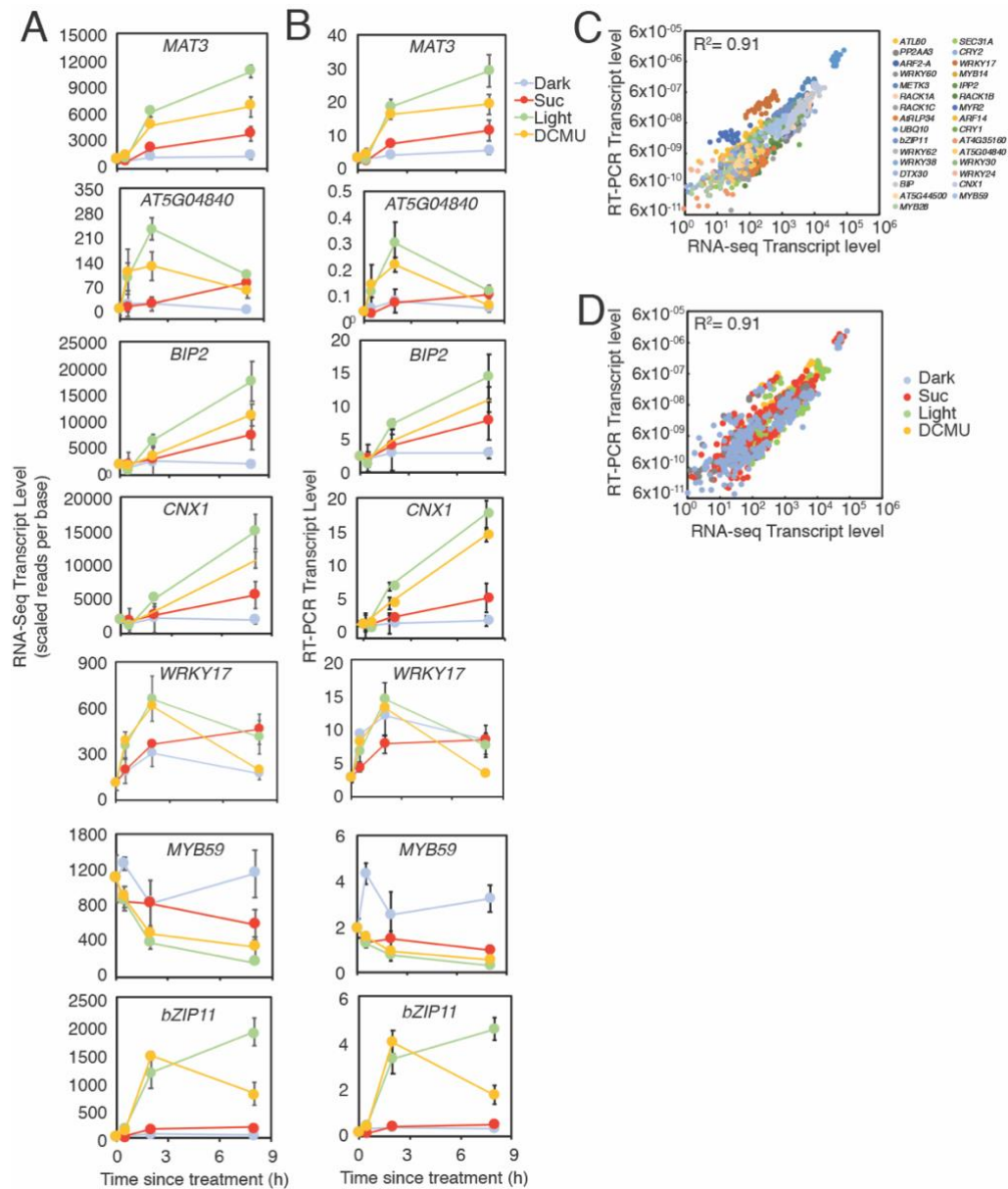
146 containing 250  $\mu$ l liquid  $\frac{1}{2}$  MS before dusk (ZT12), wrapped in aluminium foil and placed in the  
147 dark for 72 h. At subjective dawn under dim green light, media was replaced with 100  $\mu$ l 100  $\mu$ M  
148 L-012, 20  $\mu$ g/ml horseradish peroxidase containing 0.01% DMSO, 10  $\mu$ M DPI, 2  $\mu$ M MV, 0.2 mM  
149 3-AT, 20  $\mu$ M VAS2870, 500  $\mu$ M apocynin or 500  $\mu$ M allopurinol. After 1 h of chemical pre-  
150 treatment 100  $\mu$ l of 60 mM sucrose or mannitol was added to each well (final sugar concentration  
151 30 mM). Luminescence was measured in the dark at 90 s intervals in a Lumistar Omega plater  
152 reader (BMG) using a 4 mm orbital well scan.

153  
154 **Luciferase luminescence assays.** For sugar-response assays, *CCR2p:LUC* seeds were sown  
155 on  $\frac{1}{2}$  MS and grown in LD. Pairs of 10 d old seedlings were transferred into 96-well luminescence  
156 plates (Greiner) containing 200  $\mu$ l  $\frac{1}{2}$  MS with agar at dusk, wrapped in foil and grown in the dark.  
157 1 mM D-luciferin, K-salt (Promega) was applied twice under dim green light. After 84 h in the dark  
158 (subjective dawn), 20  $\mu$ l of 0.5% (v/v) DMSO, 50  $\mu$ M DPI, 10  $\mu$ M MV or 1 mM 3-AT was applied to  
159 seedlings under dim green light, 1 h before addition of 30  $\mu$ l of 30 mM mannitol or sucrose. For  
160 the dose response curves, seedlings were transferred under dim green light to  $\frac{1}{2}$  MS media  
161 containing DMSO, DPI, VAS2870, apocynin or allopurinol 12 h before application of sugar at  
162 subjective dawn. Luminescence was measured in the dark at 1 h intervals in a Lumistar Omega  
163 plate reader (BMG) using a 4 mm orbital well scan.

164  
165 To measure circadian rhythms, clusters of 5 seeds were sown on  $\frac{1}{2}$  MS and grown in LD.  
166 Clusters of 7 d old seedlings were transferred at dawn to  $\frac{1}{2}$  MS containing 30 mM mannitol or  
167 sucrose with 0.1% (v/v) DMSO, 10  $\mu$ M DPI, 2  $\mu$ M MV or 0.2 mM 3-AT. 1 mM D-luciferin, K-salt  
168 (Promega) was applied to seedlings twice prior to imaging. Luciferase was imaged in 10 min  
169 integrations following 120 s of dark at 1 hr intervals with an HRPCS5 intensified CCD camera  
170 (Photek) fitted with LB3 red (640 nm) and blue (470 nm) LED arrays providing light at 60  $\mu$ mol m<sup>-2</sup>  
171 s<sup>-1</sup> for 1 LD followed by continuous low light at 10  $\mu$ mol m<sup>-2</sup> s<sup>-1</sup>. Luminescence counts were  
172 extracted from ROIs using Image32 software (Photek) and circadian rhythms were analysed by  
173 Fast Fourier Transform Non-linear Least Squares using Biodare2 (16).

174  
175 **Sugar quantification.** Seedlings were grown as for the RNA-Seq experiment or pairs of seeds  
176 were sown on  $\frac{1}{2}$  MS and grown in LD. Seven d old seedlings were wrapped in foil at dusk and  
177 grown in the dark. After 72 h, seedlings were transferred under dim green light into 96 well plates  
178 containing  $\frac{1}{2}$  MS with 0.1% DMSO or 10  $\mu$ M DPI. At subjective dawn, seedlings were treated with  
179 30  $\mu$ l 30 mM mannitol or sucrose. 30 seedlings were harvested per biological replicate, frozen in  
180 liquid N and stored at -80°C until processing. Soluble sugars were extracted in 80% (v/v) ethanol  
181 measured using a Sucrose/Glucose/Fructose calorimetric assay kit (Megazyme) scaled down for  
182 96-well plates.

183  
184



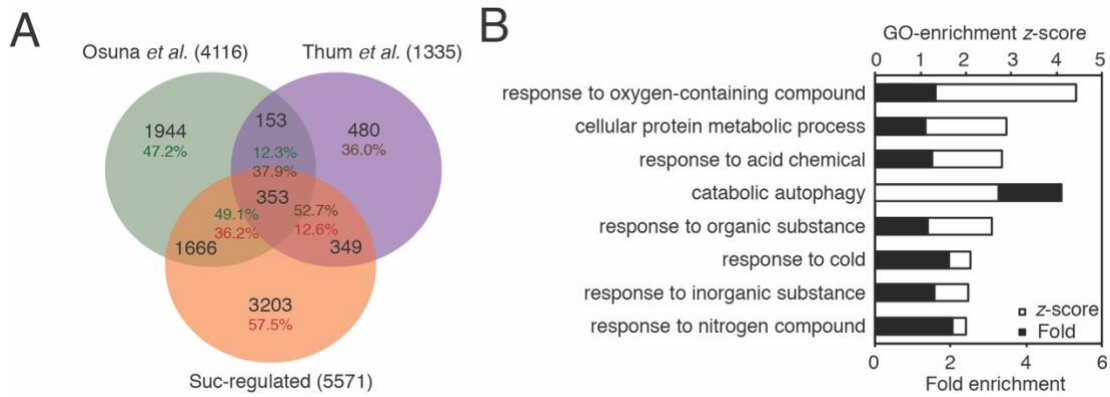
186

187 **Fig. S1.** Quality control of RNA-seq transcript data. (A) and (B) comparison of quantification of 8  
 188 representative marker genes determined by RNA-Seq (A) and qRT-PCR relative to geometric  
 189 mean of *PP2AA3* and *IPP2* (B) (means  $\pm$  SD,  $N = 3$ ). (C) and (D) comparison of quantification of  
 190 31 transcripts by qRT-PCR (PCR efficiency<sup>-C<sub>t</sub></sup>) and RNA-seq (scaled reads per base). Plots are  
 191 the same data coloured by transcript (C) or treatment (D). Values are individual biological  
 192 replicates.

193

194

195

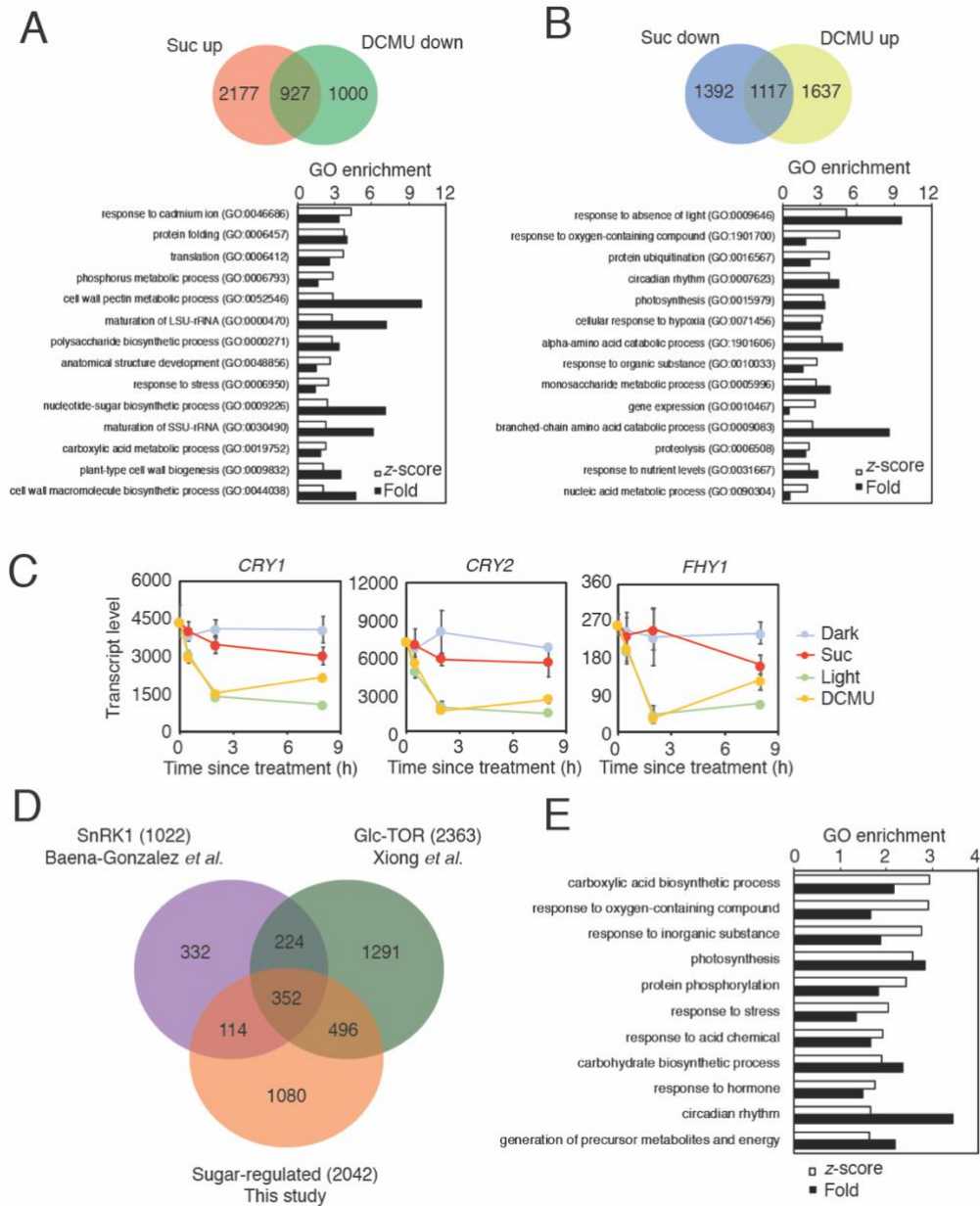


196

197 **Fig. S2.** Defining the light-independent sugar-regulated transcriptome in *Arabidopsis* shoots. (A)  
198 Comparison of genes identified as sugar-regulated in the dark in this study with two previous  
199 studies (17, 18). (B) Gene Ontology enrichment of 2772 differentially-expressed genes after 2 h  
200 treatment with mannitol or sucrose in the dark showing GO categories with a z-score > 2.

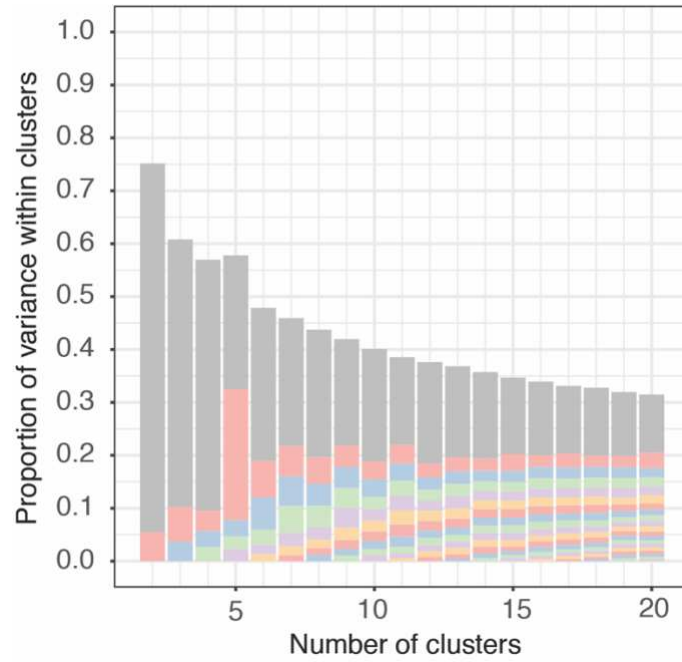
201

202



205 **Fig. S3.** Light-independent sugar-regulated genes in Arabidopsis. (A) Gene Ontology enrichment  
 206 of 927 genes that are up-regulated by sucrose in the dark and down-regulated by DCMU in the  
 207 light. (B) Gene Ontology enrichment of 1117 genes that are down-regulated by sucrose in the  
 208 dark and up-regulated by DCMU in the light. Fold-enrichment and z-score are plotted on the  
 209 same scale. (C) RNA-seq transcript level of light-signalling genes identified as down-regulated by  
 210 sucrose and up-regulated by DCMU. (D) Comparison of 2042 genes identified as sugar-regulated  
 211 in (A) and (B) to genes reported as regulated by SnRK1 (19) and TOR (20). (E) Gene Ontology  
 212 enrichment of 1080 sugar-regulated genes not previously identified as SnRK1- or TOR-regulated  
 213 showing GO categories with a z-score > 2. Fold-enrichment and z-score are plotted on the same  
 214 scale.  
 215



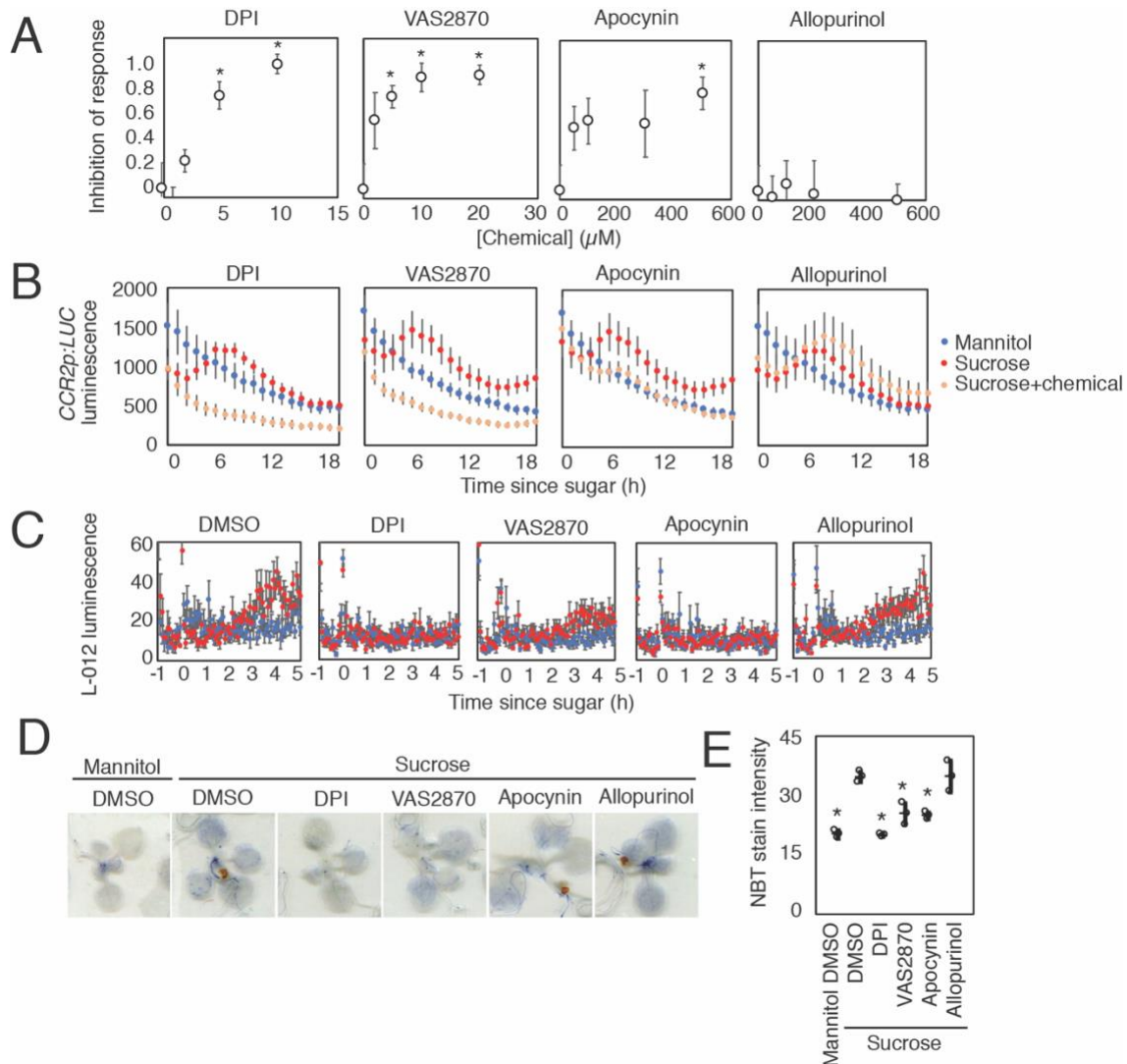


216

217 **Fig. S4.** Optimisation of gene clustering. Elbow plot of percentage of total variance within clusters  
 218 for clustering runs with k=2 to k=20. Grey is cluster with largest variance, usually representing  
 219 unclustered genes.

220

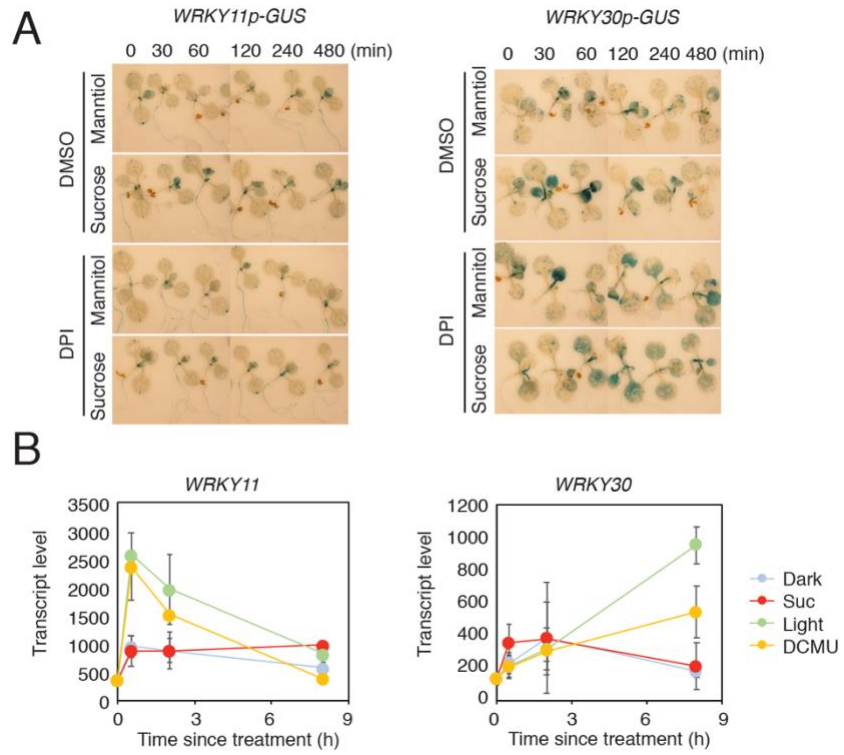
221



223  
224  
225  
226  
227  
228  
229  
230  
231  
232  
233  
234  
235  
236  
237  
238  
239

**Fig S5.** Effects of NADPH oxidase inhibitors. (A) Inhibition of response of luciferase luminescence to 30 mM sucrose in dark-adapted *CCR2p:LUC* seedlings by DPI, VAS2870, apocynin or allopurinol in the presence of four concentrations of each chemical inhibitor or DMSO (means  $\pm$  SEM,  $N = 6$ ; \*  $P < 0.05$  from DMSO; Bonferroni-corrected  $t$ -test). (B) Luciferase luminescence in dark-adapted *CCR2p:LUC* seedlings treated with 30 mM mannitol or sucrose in the presence of 0.1% DMSO, 10  $\mu\text{M}$  DPI, 20  $\mu\text{M}$  VAS2870, 500  $\mu\text{M}$  apocynin or 500  $\mu\text{M}$  allopurinol (means  $\pm$  SEM,  $N = 6$ ). (C) L-012 luminescence in dark-adapted Col-0 treated with 30 mM mannitol or sucrose in the presence of DMSO, 10  $\mu\text{M}$  DPI, 20  $\mu\text{M}$  VAS2870 or 500  $\mu\text{M}$  apocynin or 500  $\mu\text{M}$  allopurinol (means  $\pm$  SEM,  $N = 12$ ). (D) Representative images and (E) quantification of NBT stains in dark-adapted Col-0 seedlings 4 h after treatment with 30 mM mannitol or sucrose in presence of 0.1% DMSO, 10  $\mu\text{M}$  DPI, 30  $\mu\text{M}$  VAS2870, 500  $\mu\text{M}$  Apocynin or 500  $\mu\text{M}$  allopurinol (means  $\pm$  SD,  $N = 3$ ; \*  $P < 0.05$  from DMSO+Sucrose ; Bonferroni-corrected  $t$ -test).

240  
241



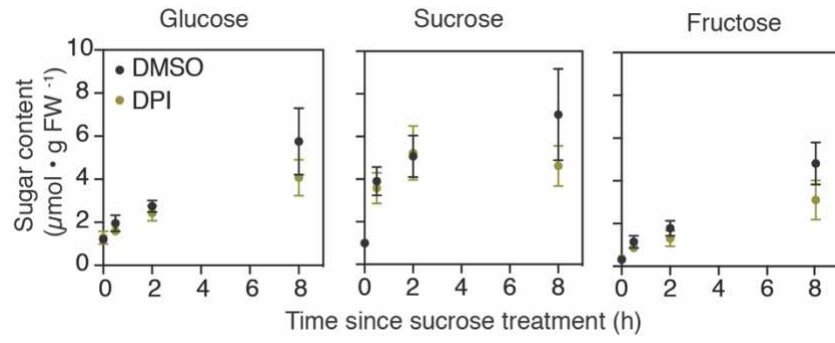
242

243

244 **Fig. S6.** Sugar and DPI affect *WRKY* promoter activity. (A) GUS stains of dark-adapted 10 d old  
245 *WRKY11p-GUS* and *WRKY30p-GUS* seedlings treated with 30 mM mannitol or sucrose, pre-  
246 treated for 30 min with DMSO or 10  $\mu$ M DPI. (B) RNA-seq transcript levels of *WRKY11* and  
247 *WRKY30* (means  $\pm$  SD,  $N = 3$ ).

248

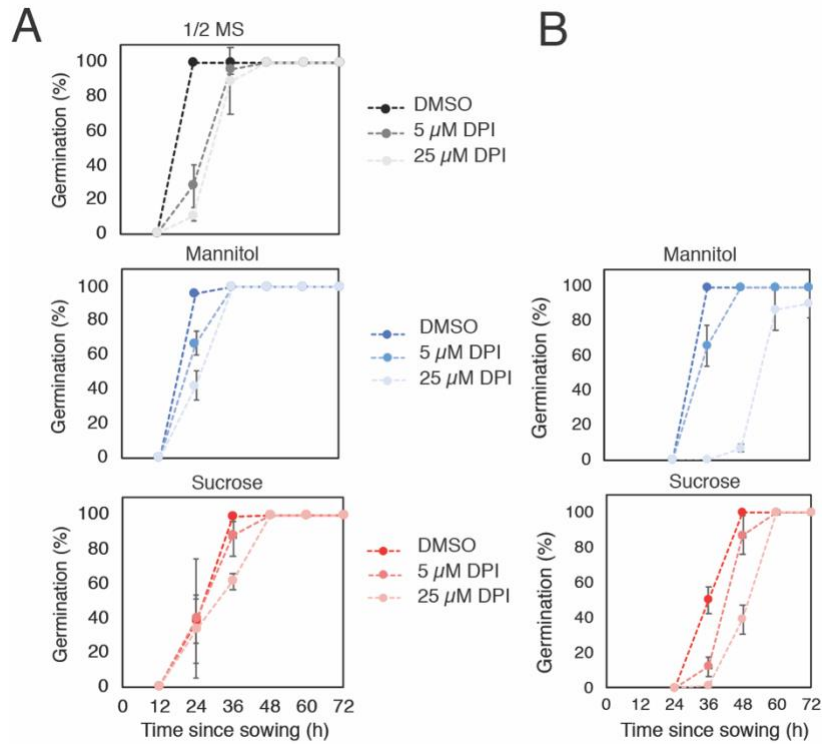
249



250

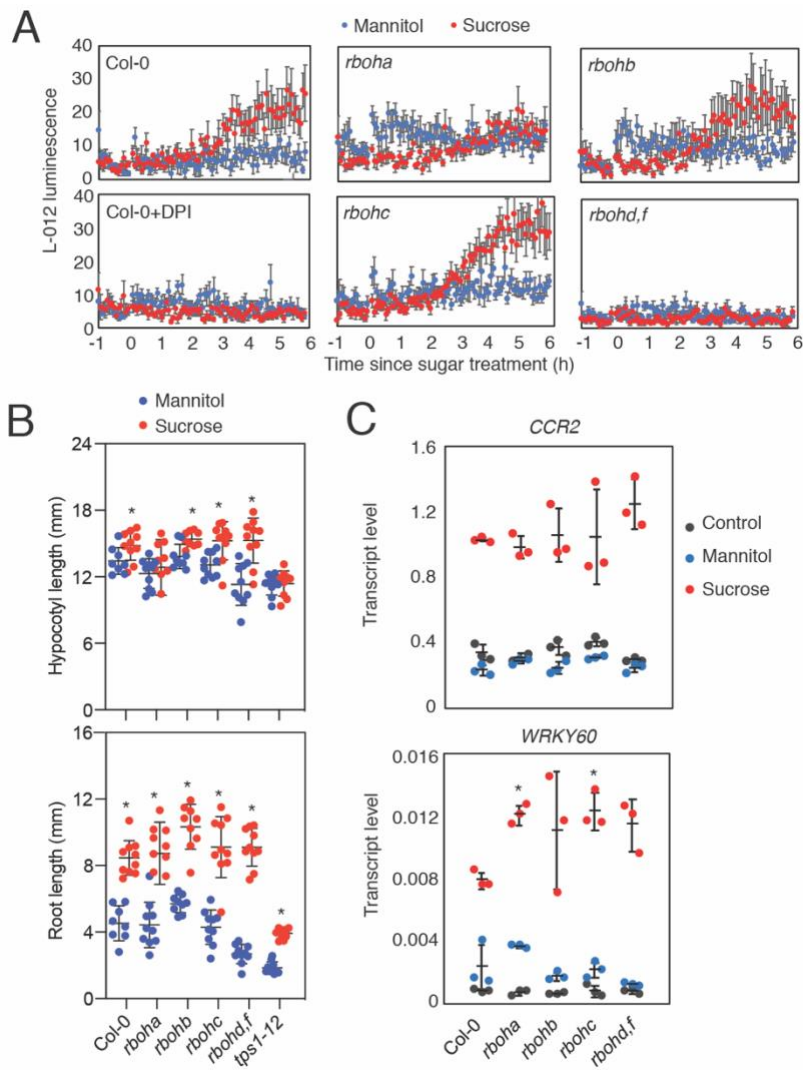
251 **Fig. S7.** Soluble sugar content in DPI-treated seedlings. Glucose, sucrose and fructose content in  
 252 dark-adapted Col-0 seedlings treated with 30 mM sucrose in the presence of 0.1% DMSO or 10  
 253 μM DPI. Values are means ± SD, *N* = 4. No significant difference was identified between DMSO  
 254 or DPI treated seedlings by *t*-test with Bonferroni correction, *P* < 0.05.

255  
 256



257

258 **Fig. S8.** Additive effects of DPI and sucrose on seed germination. (A) Percentage of germinated  
 259 (A) non-dormant Col-0 seeds following 2 d chilling at 4°C or (B) dormant seeds without chilling  
 260 sown on 1/2 MS with or without 30 mM mannitol or sucrose and 0.1% DMSO or DPI. Values are  
 261 mean ± SD of four independent seed populations.  
 262  
 263

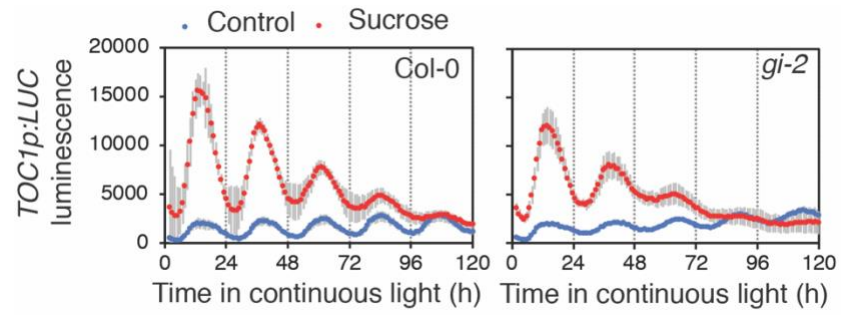


265

266 **Fig. S9.** NADPH oxidases contribute redundantly to sugar responses. (A) L-012 luminescence in  
 267 dark-adapted Col-0 (with or without 10  $\mu$ M DPI), *rboha*, *rbohbb*, *rbohbc* and *rbohbd rbohbf* seedlings  
 268 after treatment with 30 mM mannitol or sucrose (means  $\pm$  SEM,  $N = 6$ ). (B) Hypocotyl length and  
 269 root length of 5 d old dark-grown Col-0, *rboha*, *rbohbb*, *rbohbc*, *rbohbd rbohbf* and *tps1-12*  
 270 seedlings grown on  $\frac{1}{2}$  MS with 30 mM mannitol or sucrose (means  $\pm$  SD,  $N = 10$ ; \*  $P < 0.05$  from  
 271 mannitol,  $t$ -test). (C) Transcript level of *CCR2* and *WRKY60*, relative to *UBQ10* in dark-adapted  
 272 Col-0 and *rboh* mutant seedlings (control) or 12 h after treatment with 30 mM mannitol or sucrose  
 273 (means  $\pm$  SD,  $N = 3$ ; \*  $P < 0.05$  from Col-0; Bonferroni-corrected  $t$ -test).

274

275



276

277

278 **Fig. S10.** Effects of ROS chemicals on circadian rhythms. Luciferase luminescence in Col-0  
 279 *TOC1p:LUC* and *gi-2 TOC1p:LUC* seedlings in continuous light with or without 90 mM sucrose  
 280 (means  $\pm$  SEM,  $N = 4$ ).

281

282

283  
284

285 **Dataset 1 (separate file).** Differentially expressed genes between Dark and Suc or Light and  
286 DCMU.

287 **Dataset 2 (separate file).** Lists of sugar-activated and sugar-repressed genes.

288 **Dataset 3 (separate file).** Gene lists and GO enrichment of 14 clusters.

289 **Dataset 4 (separate file).** Complete GO enrichment map of top 15 terms from 14 gene clusters.

290 **Dataset 5 (separate file).** Gene lists and phase analysis of ROS-regulated genes.

291 **Dataset 6 (separate file).** Primer sequences.

292

## 293 SI References

294

- 295 1. M. J. Haydon, O. Mielzcarek, F. C. Robertson, K. E. Hubbard, A. a. R. Webb,  
296 Photosynthetic entrainment of the Arabidopsis circadian clock. *Nature* **502**, 689–692  
297 (2013).
- 298 2. L. D. Gómez, A. Gilday, R. Feil, J. E. Lunn, I. A. Graham, AtTPS1-mediated trehalose 6-  
299 phosphate synthesis is essential for embryogenic and vegetative growth and  
300 responsiveness to ABA in germinating seeds and stomatal guard cells. *Plant J.* **64**, 1–13  
301 (2010).
- 302 3. M. J. Haydon, *et al.*, Vacuolar nicotianamine has critical and distinct roles under iron  
303 deficiency and for zinc sequestration in Arabidopsis. *Plant Cell* **24**, 724–37 (2012).
- 304 4. A. G. Lai, *et al.*, CIRCADIAN CLOCK-ASSOCIATED 1 regulates ROS homeostasis and  
305 oxidative stress responses. *Proc. Natl. Acad. Sci.* **109**, 17129–17134 (2012).
- 306 5. R. Patro, G. Duggal, M. I. Love, R. A. Irizarry, C. Kingsford, Salmon provides fast and  
307 bias-aware quantification of transcript expression. *Nat. Methods* **14**, 417–419 (2017).
- 308 6. H. Pimentel, N. L. Bray, S. Puente, P. Melsted, L. Pachter, Differential analysis of RNA-  
309 seq incorporating quantification uncertainty. *Nat. Methods* **14**, 687–690 (2017).
- 310 7. K. Van den Berge, C. Sonesson, M. D. Robinson, L. Clement, stageR: A general stage-  
311 wise method for controlling the gene-level false discovery rate in differential expression  
312 and differential transcript usage. *Genome Biol.* **18**, 1–14 (2017).
- 313 8. C. Y. Cheng, *et al.*, Araport11: a complete reannotation of the Arabidopsis thaliana  
314 reference genome. *Plant J.* **89**, 789–804 (2017).
- 315 9. R. J. Kinsella, *et al.*, Ensembl BioMarts: A hub for data retrieval across taxonomic space.  
316 *Database* **2011**, 1–9 (2011).
- 317 10. S. Durinck, P. T. Spellman, E. Birney, W. Huber, Mapping identifiers for the integration of  
318 genomic datasets with the R/ Bioconductor package biomaRt. *Nat. Protoc.* **4**, 1184–1191  
319 (2009).
- 320 11. H. Mi, *et al.*, Protocol Update for large-scale genome and gene function analysis with the  
321 PANTHER classification system (v.14.0). *Nat. Protoc.* **14**, 703–721 (2019).
- 322 12. J. M. Ruijter, *et al.*, Amplification efficiency: Linking baseline and bias in the analysis of  
323 quantitative PCR data. *Nucleic Acids Res.* **37** (2009).
- 324 13. F. Pedregosa, *et al.*, Scikit-learn: Machine learning in Python. *J. Mach. Learn. Res.* **12**,  
325 2825–2830 (2011).
- 326 14. G. Yu, L. G. Wang, Y. Han, Q. Y. He, ClusterProfiler: An R package for comparing  
327 biological themes among gene clusters. *OMICS* **16**, 284–287 (2012).
- 328 15. Á. Román, J. F. Golz, A. A. R. Webb, I. A. Graham, M. J. Haydon, Combining GAL4 GFP  
329 enhancer trap with split luciferase to measure spatiotemporal promoter activity in  
330 Arabidopsis. *Plant J.* **102**, 187–198 (2020).
- 331 16. T. Zielinski, A. M. Moore, E. Troup, K. J. Halliday, A. J. Millar, Strengths and Limitations of



- 332 Period Estimation Methods for Circadian Data. *PLoS One* **9**, e96462 (2014).  
333 17. K. E. Thum, M. J. Shin, P. M. Palenchar, A. Kouranov, G. M. Coruzzi, Genome-wide  
334 investigation of light and carbon signaling interactions in Arabidopsis. *Genome Biol.* **5**,  
335 R10 (2004).  
336 18. D. Osuna, *et al.*, Temporal responses of transcripts , enzyme activities and metabolites  
337 after adding sucrose to carbon-deprived Arabidopsis seedlings. *Plant J.* **49**, 463–491  
338 (2007).  
339 19. E. Baena-González, F. Rolland, J. M. Thevelein, J. Sheen, A central integrator of  
340 transcription networks in plant stress and energy signalling. *Nature* **448**, 938–42 (2007).  
341 20. Y. Xiong, *et al.*, Glucose-TOR signalling reprograms the transcriptome and activates  
342 meristems. *Nature* **496**, 181–6 (2013).  
343